RIGA TECHNICAL UNIVERSITY

Sergey Kravchenko

DEVELOPMENT OF ELECTRIC PROPULSION THRUSTERS COOLING SYSTEMS FOR PERSPECTIVE SPACECRAFTS

Summary of the Doctoral Thesis

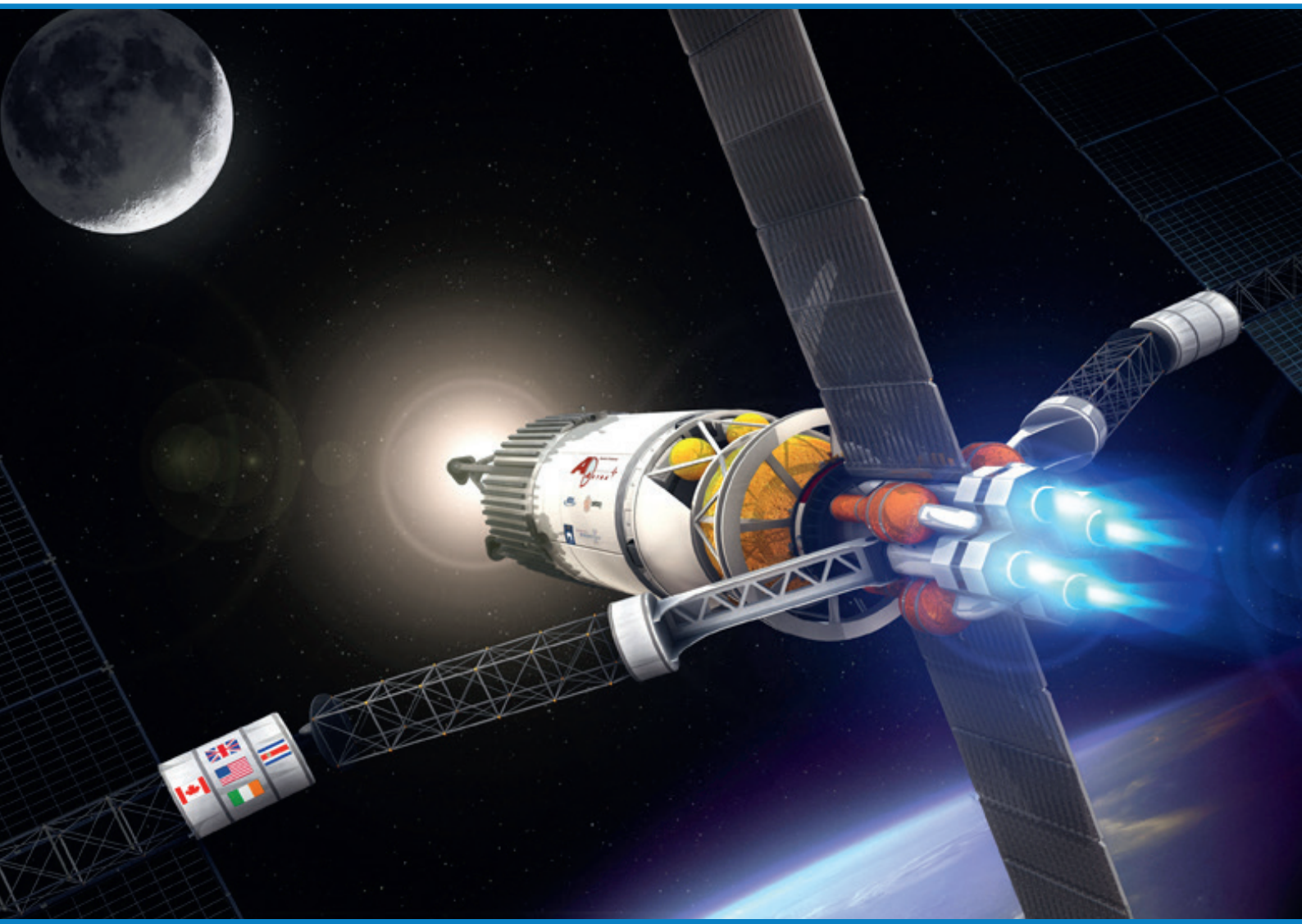

RTU Press
Riga 2021

RIGA TECHNICAL UNIVERSITY
Faculty of Mechanical Engineering, Transport and Aeronautics
Institute of Aeronautics

Sergey Kravchenko
Doctoral Student of the Study Program "Transport"

DEVELOPMENT OF ELECTRIC PROPULSION THRUSTERS COOLING SYSTEMS FOR PERSPECTIVE SPACECRAFTS

Summary of the Doctoral Thesis

Scientific supervisor
Professor Dr. habil. sc. ing.
VLADIMIRS ŠESTAKOVS

RTU Press
Riga 2021

Kravchenko, S. Development of Electric Propulsion Thrusters Cooling Systems for Perspective Spacecrafts. Summary of the Doctoral Thesis. Riga: RTU Press, 2021. 49 p.

Published in accordance with the decision of the Promotion Council "RTU P-22" of 6 November 2020, Minutes No. 04030-9.18.1/3.

Cover photo by *Ad Astra Rocket Company*.

https://doi.org/10.7250/9789934225949
ISBN 978-9934-22-593-2 (print)
ISBN 978-9934-22-594-9 (pdf)

DOCTORAL THESIS PROPOSED TO RIGA TECHNICAL UNIVERSITY FOR THE PROMOTION TO THE SCIENTIFIC DEGREE OF DOCTOR OF SCIENCE

To be granted the scientific degree of Doctor of Science (*Ph. D.*), the present Doctoral Thesis has been submitted for a remote defence at the open meeting of RTU Promotion Council on April 23, 2021 at 14.00.

OFFICIAL REVIEWERS

Profesor Dr. habil. sc. ing. Vitālijs Pavelko
Riga Tehnical University, Latvia

Profesor Dr. habil. sc. ing. Aleksandrs Andronovs
St. Petersburg State University of Civil Aviation, Russia

Profesor Dr. habil. sc. ing. Zbigniew Koruba
Kielce University of Technology, Poland

DECLARATION OF ACADEMIC INTEGRITY

I hereby declare that the Doctoral Thesis submitted for the review to Riga Technical University for the promotion to the scientific degree of Doctor of Science (*Ph. D.*) is my own. I confirm that this Doctoral Thesis had not been submitted to any other university for the promotion to a scientific degree.

Sergey Kravchenko ……. (signature)

Date: ……

The Doctoral Thesis has been written in English. It consists of an Introduction; 7 chapters; Summary and Conclusions; 42 figures; 4 tables; 2 appendices; the total number of pages is 134. The Bibliography contains 72 titles.

TABLE OF CONTENTS

INTRODUCTION

Subject relevance of the Thesis

Over the past 20 years, the pace of space exploration has slowed significantly compared to the period between the fifties and the nineties of the twentieth century. There are two main reasons that can be distinguished for this process.

- Exhaustion of the need for qualitative development of space research of near-Earth space, since the next step should be the technological development of near-Earth space. But there are no technologies whose development on the Earth orbit would be economically justified today due to the high cost of existing methods of launching into orbit a spacecraft with technological materials and equipment.
- Inability at present to initiate any qualitative development of interplanetary research and development missions due to the extremely low ratio of the mass of the mission payload to the mass of the mission spacecraft equipped with traditional chemical engines. This low ratio is a consequence of the small specific impulse of traditional chemical engines, which have an appropriate thrust to deliver the necessary payload to the Earth orbit. But low specific impulse is the reason for long-term missions and very small payload reaching the celestial bodies of the Solar system.

A solution to the problem of increasing a specific impulse has existed since the 60s of the twentieth century. This is the reason for a widespread implementation of electric rocket thrusters, i.e., Electric Propulsion Thrusters (EPTs), the most promising models of which today have a specific impulse that is more than 20 times higher than that of modern chemical rocket thrusters.

The implementation of EPTs creates an opportunity for a new space exploration era, i.e., the widespread development of the Moon, Terrestrial Planets (Mars, Venus, Mercury) and the Solar system as a whole for the benefit of all mankind.

In addition, socially useful space products with significant functional capabilities and a corresponding market demand in the long term of 20–30 years can only be provided by sufficiently large and heavy satellites that need powerful and lightweight power plants, that is, powerful EPTs.

Therefore, the priority in this area, corresponding to the demands of the space market, is the creation of a sufficiently powerful, reliable and durable EPT.

The main problem limiting the mass implementation and use of EPTs is the limitation of their power due to thermal destruction of the thruster structure. Therefore, the most effective solution, which will significantly increase the EPT thrust without thermal destruction, in the near future is the creation and implementation of an effective cooling system for thruster structural elements.

This determines the relevance of this research.

Research object – a promising high-powered electric propulsion (rocket) thruster (EPT).

Research subject – cooling systems of an electric rocket thruster structure.

The aim of the given research – development of theoretical, methodological and experimental approaches to the EPT lifespan and efficiency extension by improving its cooling system.

Research methods – formalization, generalization, physical and mathematical modeling, experiment, comparison, as well as methods of the theory of algorithms and applied programming.

Scientific novelty

1. Multivariate physical and mathematical model of the EPT cooling system.
2. Step-by-step methodological manual and algorithm for calculating the EPT cooling system parameters.
3. A software package allowing calculation of EPT cooling system parameters with varying initial data and boundary conditions.

Results of research

1. The analysis of modern electric propulsion (rocket) thrusters (EPTs) and their promising developments, their advantages and disadvantages in relation to rocket thrusters using the energy of expansion of gases, which are the products of combustion of rocket fuel. The main operational requirement of a promising spacecraft is the creation of a sufficiently powerful EPT, however, today no such thruster exists. The most powerful models of mass-produced EPT have a thrust in the range of 0.05–0.10 N. The main problem on the way of their wide development and implementation is the problem of thermal destruction of the structures of a powerful EPT.
2. Based on an analysis of theoretical mechanisms of energy conversion in Electric Propulsion Thrusters, a methodological manual has been developed for assessing the processes of destruction of the EPT structures.
3. A multivariate physical and mathematical model of the EPT cooling system was developed based on the heat balance equation and EPT structural diagram, which includes three elements: a heat-receiving subsystem, a heat transfer subsystem, and a heat dissipation subsystem. When developing the mathematical model, the method of step-by-step problem solving was used.
4. On the basis of the physical and mathematical model, a step-by-step methodological manual and algorithm for calculating the EPT cooling system parameters have been developed.

5. An experimental Electric Propulsion Thruster with a cooling system developed by the author was manufactured and tested on a specially designed experimental facility and test bench.
6. A series of experiments was performed with a Magneto Plasma Dynamic Ion-Plasma Thruster with its own magnetic field without a cooling system (MPDO) and with a cooling system developed by the author.
7. Based on the analysis of the experiment results, the author provided an evidence that the cause of overheating and destruction of the thruster anode is electronic bombardment of the anode.
8. The correctness of the obtained experimental results was assessed by the author both on the basis of verification – a comparison of the results obtained at several objects, and a comparison of the results obtained by calculation and experiment.

Practical significance

- A software package which allows making calculations of the EPT cooling system parameters with varying initial data and boundary conditions.
- Practical recommendations that can be applied to design electric propulsion thrusters with cooling systems.

The provisions that are suggested for defense

1. The physical and mathematical model of the EPT cooling system.
2. The methodological manual and algorithm for calculating parameters of EPT cooling systems.
3. The hypothesis of the processes development of overheating and destruction of the EPT electrode system.
4. Software package, which allows for making calculations of EPT cooling systems parameters with varying initial data and boundary conditions.

Approbation

This Thesis and the development of the MPDE EPT were commissioned by *Cryogenic and vacuum systems* Ltd. as part of the creation of a promising budget vehicle for transportation between lunar objects within the framework of international project “Moon Village” developed under the auspices of the ESA.

Participation in international scientific conferences

1. Space Industry Day 2019, Latvia, Riga, 20 March 2019, report: “Electric Propulsion Thrusters Testing Approach”, authors: S. Kravchenko, N. Panova.

2. 22nd International Scientific Conference TRANSPORT MEANS 2018, Lithuania, Trakai, 3–5 October 2018, report: “Evaluating the Efficiency of Spacecraft Electric Thruster”, authors: S. Kravchenko, A. Urbah.
3. Space Tech Expo Europe 2017, Technology Forum, Germany, Bremen, 24–26 October 2017, report: “Electric Thrusters Thermal Vacuum Testing”, author: S. Kravchenko.
4. Riga Technical University 58th International Scientific Conference, Latvia, Riga, 12–18 October 2017, report: “Development of Cooling System of Ion-Plasma Engines”, authors: S. Kravchenko, A. Urbah.
5. European Planetary Science Congress 2017, Latvia, Riga, 17–22 September 2017, report: “Small interplanetary spacecraft and their electric propulsion systems testing approach”, author: S. Kravchenko.
6. 5th International Scientific Conference of Ventspils International Radio Astronomy Centre, Latvia, Ventspils, 23–24 August 2017, report: “METAMORPHOSIS – the space testing facility from Ventspils”, authors: S. Kravchenko, N. Panova, M. Cēbere.

Unfortunately, a lot of scientific conferences from the end of 2019 were cancelled or postponed due to COVID-19 (e.g., European Conference on Spacecraft Structures, Materials and Environmental Testing ECSSMET2020).

Publications

1. Kravchenko, S., Kuleshov, N., Shestakov, V. Approach to mathematical modeling of the thermal stress of ion-plasma thrusters. Article accepted by the Editorial Board of *Transport and Aerospace Engineering* in May 2020.
2. Kravchenko, S., Kuleshov, N., Shestakov, V. Ion-Plasma Thrusters Thermal Balance Estimation. *Journal of Multidisciplinary Engineering Science and Technology (JMEST)*, 2020, vol. 7, no. 4, pp. 11666–11674. e-ISSN 2458-9403.
3. Kravchenko, S., Urbahs, A. Evaluating the Efficiency of Spacecraft Electric Thruster Operation. In: *Transport Means 2018: Proceedings of the 22th International Scientific Conference*, Lithuania, Trakai, 3–5 October 2018. Kaunas: Kaunas University of Technology, 2018, pp. 983–986. ISSN 1822-296X. e-ISSN 2351-7034.
4. Urbahs, A., Kravchenko, S. Development of Cooling Systems of Ion-Plasma Engines. In: *Riga Technical University 58th International Scientific Conference: Programme*, Latvia, Riga, 12–18 October 2017. Riga: RTU, 2017, pp.184-184. ISBN 978-9934-22-001-2.
5. Kravchenko, S., Panova, N., Cēbere, M. METAMORPHOSIS – the Space Testing Facility from Ventspils. In: *Space Research Review, vol. 5*, Latvia, Ventspils, 23–24 August 2017. Ventspils: Ventspils University of Applied Sciences, 2018, pp. 98–105 ISBN 978-9984-648-89-7.

6. Urbahs, A., Visockiene, Y., Liu, Y., Carjova, K., Kravchenko, S. Human-In-The-Loop Remote Piloted Aerial Systems in the Environmental Monitoring. *Transport and Aerospace Engineering*, 2016, vol. 3, iss. 1, pp. 91–100. ISSN 2255-968X. e-ISSN 2255-9876. DOI:10.1515/tae-2016-0011.
7. Kravchenko, S., Nesterov, S., Romanko, V., Testoedov, N., Khalimanovich, V., Khristich, V. Approaches to Creation of Complex Systems for Trying-out and Testing of Spacecrafts. In: *Herald of the Bauman Moscow State Technical University, Series "Mechanical Engineering",* Special publication no. 1 "Refrigeration and Cryogenic Technology, Systems of Air Conditioning and Life Support", 2013, pp. 149–175, UDK 621.528.1 ISSN 0236-3941, republished in: *Engineering Journal: Science and Innovations*, 2013, Issue #1(13)/2013, ISSN 2308-6033. DOI: 10.18698/2308-6033-2013-1-598.
8. Kravchenko, S., Nesterov, S., Testoedov, N., Khalimanovich, V., Khristich, V. *Calculation and Design of Space Simulating Facilities Cryogenic Shrouds.* Moscow: Novella, 2013. 89 p. ISBN 978-5-904463-37-3.
9. Kravchenko, S. V., Nesterov, S. B., Michalkin, V. M., Testoedov, N. A., Khalimanovich, V. I., Khristich, V. V., Sharov, A. K. Preparation of Initial Data to Calculate and Design Cryogenic Systems for Thermal Vacuum Spacecraft Testing. In: *Vacuum Equipment, Materials and Technology: Proceedings of the VIII International Conference Proceedings,* Moscow, Sokolniki Culture & Exhibition Centre, 2013, April 16–18 / Ed. Professor *Dr. habil. sc. ing.* Nesterov S. B., Russia, Moscow, 16–18 April 2013. Moscow: Novella, 2013, pp. 288–295. ISBN 978-5-904463-36-6.
10. Kravchenko, S. V., Nesterov, S. B., Michalkin, V. M., Testoedov, N. A., Khalimanovich, V. I., Khristich, V. V., Sharov, A. K. Creation of Comprehensive Systems for Thermal Vacuum Testing of Space Equipment. In: *Vacuum Equipment, Materials and Technology: Proceedings of the VIII International Conference*, Moscow, Sokolniki Culture & Exhibition Centre, 2013, April 16–18 / Ed. Professor *Dr. habil. sc. ing.* Nesterov S. B., Russia, Moscow, 16-18 April, 2013. Moscow: Novella, 2013, pp. 275–287. ISBN 978-5-904463-36-6.
11. Kravchenko, S. V., Nesterov, S. B., Romanko, V. A., Testoedov, N. A., Halimanovich, V. I., Hristich, V. V. *Approaches of the spacecraft testing facilities development.* Moscow: Novella publishing, 2012. ISBN 978-5-904463-30-4, 32 p.

The structure of the Thesis

The Doctoral Thesis consists of an introduction, seven chapter summary and conclusions. It comprises 134 pages, including 4 tables and 42 figures, 72 literature references, and 2 appendices.

1. ANALYSIS OF ELECTRIC ROCKET THRUSTERS (EPT) CURRENT DEVELOPMENT STATE, THEIR ADVANTAGES AND DISADVANTAGES

The definition of Electric Propulsion given by the European Space Agency is as follows: Electric Propulsion (EP) is a class of space propulsion that makes use of electrical power to accelerate a propellant by different possible electrical and/or magnetic means [3].

The advantages of EPTs:

- the lifespan (resource) is hundreds of times greater than that of chemical rocket engines. E.g., NASA confirms the continuous operation time of the EPT *NEXT* ion propulsion system for a failure of more than 51 000 hours, and the *Deep Space 1* spacecraft overcame more than 262 million km with the *NSTAR* EPT, and its velocity increase due to the operation of the electric propulsion system was more than 10 km/s [5];
- the specific impulse of modern EPTs is ten times greater than the specific impulse of chemical engines [6];
- the separation in the EPT of a source of energy and a working fluid overcomes the limitation inherent in chemical engines – the need in great amount of oxidizer and propellant.

Electric propulsion thrusters are extremely flexible systems operational processes in which are very sensitive even to a small change in parameters. In EPTs of various types, depending on the specific task, different mechanisms of the working fluid acceleration can be combined in different ways.

Today, there is a wide variety of EPTs, as they are developed based on various scientific and technical principles, the main ones of which are the following.

- The principle of electrodynamic plasma acceleration, proposed and experimentally justified in 1956–1957 by academician Lev A. Artsimovich and his associates, which laid the foundation for accelerators of various classes – pulsed EPTs on gaseous and solid working fluids, stationary high-current Magneto Plasma Dynamic EPTs.
- The principle of ion acceleration in a magnetized plasma with azimuthal electron drift. This principle is applied in thrusters with an anode layer and in Hall-effect thrusters.
- The principle of a plasma-ion thruster proposed by Professor Harold R. Kaufman (USA). In this thruster, ions are also accelerated by a longitudinal electric field, however, unlike the thruster with an anode layer, they are preliminarily pulled from a plasma discharge with electrons oscillating in a longitudinal magnetic field. Plasma-ion thruster has a high efficiency and lifespan, but loses to the thruster with the anode layer in versatility and range of performance variation.
- The principle of electrodynamic acceleration of mass, proposed in 1975–1977 by professor Gerard K. O'Neill (USA) in a Mass Driver demonstrator. Such thrusters also use energy transmitted to the spacecraft in the form of a well-focused microwave beam from the Earth or spacecraft.

EPTs developed on basis of these principles are enormously diverse and the EPT classification has not been established to date. Several works written on the subject present different systems, which are utilized to classify the EPTs based on their features.

Among the classification systems that most fully reflect the current European level and state in the field of research and development of EPT is the ESA classification proposed by the “Electric Propulsion Innovation & Competitiveness” (EPIC).

This classification is based on the division according to the principle of action and the main elements of the thruster structure. Within the framework of EPIC, the following EPT classification is proposed [10], which includes 11 main classes of thrusters:

1. Gridded Ion Engines (GIE);
2. Hall Effect Thrusters (HET);
3. High Efficiency Multistage Plasma Thrusters (HEMPT);
4. Pulsed Plasma Thrusters (PPT);
5. Magneto Plasma Dynamic Thrusters (MPDT or MPD);
6. Quad Confinement Thrusters (QCT);
7. Resistojet;
8. Arcjet;
9. Field Emission Electric Propulsion Thrusters (FEEP);
10. Colloid and Electrospray Thrusters (CET);
11. Electrode-less Thrusters (ELT).

However, this classification can be considered too cumbersome. Therefore, based on the analysis, author proposed to classify the electric propulsion by the prevailing particle acceleration mechanism. Then the electric propulsion, in which the operational processes differ in principle, can be divided into 3 classes and presented in the form of a diagram (Fig. 1.1).

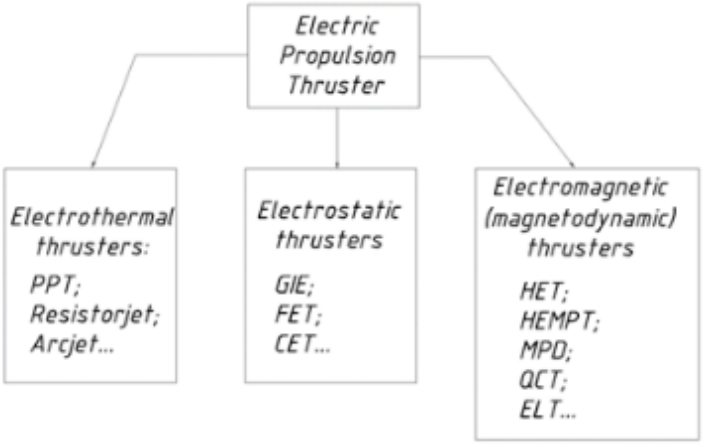

Fig. 1.1. Proposed EPT classification.

The three classes are as follows:

- Electrothermal thrusters;
- Electrostatic thrusters;
- Electromagnetic (Magneto Dynamic) thrusters.

In accordance with the proposed diagram, all thrusters which use thermodynamic principles of working fluid internal energy increasing for particle acceleration can be considered as electrothermal thrusters. All types of this class use neutral plasma for acceleration. In turn, electrothermal thrusters are classified by the type of gas discharge: electric arc, resistive jet and induction thrusters. They constitute the first class of EPTs in accordance with the proposed classification. Among them are EPIC Pulsed Plasma Thrusters (PPT), Resistojet, Arcjet.

To the second class belong the Electrostatic thrusters. Electrostatic thrusters include ionic (including colloidal) thrusters, in which particles acceleration is used due to Coulomb force action. Electrostatic thrusters can be divided according to the features of organization of the ionization and acceleration zones for electrostatic thrusters with an extended ionization and acceleration zone and for thrusters with a narrow ionization and acceleration zone.

Thrusters with a narrow ionization and acceleration zone are also divided into single-stage or multi-stage thrusters by the number of zones or stages of ionization and acceleration. Such class includes Gridded Ion Engines (GIE), Field Emission Electric Propulsion Thrusters (FEEP), Colloid and Electrospray Thrusters (CET).

The EPTs of the third class – Electromagnetic (Magneto Dynamic) thrusters, use Lorentz force for particle acceleration. In some thruster types of this class Lorentz force is combined with Coulomb force as an additional mechanism of particles acceleration. This class includes Hall-Effect Thrusters (HET), High Efficiency Multistage Plasma Thrusters (HEMPT), Magneto Plasma Dynamic Thrusters (MPDT), Quad Confinement Thrusters (QCT) and Electrode-less Thrusters (ELT) according to EPIC classification.

The basic characteristics of EPT, as well as rocket thrusters of other types [3]–[7]

Thrust, commonly referred to as *T*, is the reaction force of "dropping" the working fluid from the jet nozzle, F_{wb}. In general, the thrust force of the thruster is formed by summing up two components, the reactive force T_{m} resulting from a change in the momentum of the working fluid jet and pressure T_{p} of the gas jet, i.e., the pressure of the working fluid exhaust jet:

$$T = T_{\text{m}} + T_{\text{p}}. \tag{1.1}$$

The value of the second term is significant for thrusters that accelerate the launch vehicle in the atmosphere, that is, operate in the high-pressure region, the task of which is to "lift" the weight of the carrier "on the jet stream" of the working fluid, as well as for other atmospheric jet engines, for example, for some jet engines of aircrafts.

Therefore, for EPT, the traction force created due to the pressure of the working fluid may not be taken into account, since due to the low mass flow rate of the working fluid and its low pressure it is several orders of magnitude lower than the reaction force of "exhaust jet" of the working fluid.

Equivalent velocity that is equal to the ratio of the thrust of the rocket thruster to the mass flow of the working fluid is determined by the expression in [3]:

$$v_{\text{eq}} = \frac{T}{G} \text{ or } v_{\text{eq}} = -v_{\text{ex}} + \frac{S}{G}\left(P_{\text{ex}} - P_{\text{atm}}\right). \tag{1.2}$$

For thrusters with a small flow rate and pressure of the working fluid the value of the second term in (1.2) is negligible, compared to the value of the first one.

Therefore, with high accuracy for the EPT, it can be assumed that $|v_{eq}| = |v_{ex}|$. Then the expression for EPT thrust is as follows:

$$T = v_{ex}G. \tag{1.3}$$

Total impulse I, imparted by the thruster to the spacecraft, is as in [3]:

$$I = mv_{eq} \text{ or } I = -mv_{ex} + \frac{mS}{G}\left(P_{ex} - P_{atm}\right). \tag{1.4}$$

The efficiency of rocket thrusters is evaluated using **specific thrust and specific impulse** indicators [3], [7].

Specific impulse I_{sp} is the amount of the momentum that is created by a rocket thruster per unit weight of the working fluid:

$$I_{sp} = \frac{I}{mg}, \tag{1.5}$$

where g is the acceleration of gravity at sea level: 9.80665 m/s^2.

Specific thrust T_{sp} is the ratio of the thrust to the weight of flow rate of the working fluid:

$$T_{sp} = \frac{T}{Gg}. \tag{1.6}$$

Specific velocity ΔV is a measure of the momentum per unit of spacecraft mass that is needed to perform a maneuver or a measure of value equal to the increment of spacecraft velocity achieved because of the thruster operation during the maneuver.

From all the above mentioned an important practical conclusion is as follows: **for satellites, performing a mission in orbit** (which are the payload of launch systems) **it is not the fuel reserve that is more important but the velocity of the expiration of the working fluid v_{ex} (or specific impulse I_{sp}) of their power plant**.

For launch vehicles the fuel reserve is of higher importance.

This conclusion is important for understanding the practical need to increase the exhaust velocity of the working fluid (specific impulse) in a spacecraft with EPT.

EPT structural breakdown mechanisms

Fundamentally, any EPT, as a complex system, can be represented in the form of three subsystems:

- a subsystem for creating a working fluid (gasification and/or ionization);
- a subsystem for accelerating the working fluid (an expanding nozzle for plasmatron thrusters or ion-plasma accelerators for ion-plasma thrusters);
- a subsystem for supporting the process of plasma formation and acceleration, which includes various types of thrusters, for example, plasma cathodes, power supplies for the discharge electrode system, accelerator system, magnetic system, devices for

regulating and stabilizing the pressure of the working fluid, its storage and transportation, other auxiliary units and instruments.

The destruction of any of these three subsystems leads to fatal thruster failure. The analysis indicates three main mechanisms of the destruction of high power EPT structures:

- thermomechanical failure due to overheating and further loss of strength, stiffness and buckling stability of the thruster mechanical structures;
- electro erosive destruction due to the occurrence of a parasitic arc micro discharge in the evaporation zone of thruster structural elements when the vapor pressure reaches the discharge ignition value in accordance with the Paschen's law;
- electro erosive destruction of structures under the influence of a stream of non-neutral plasma of the working fluid of the thruster.

The cause of the first two destruction mechanisms is overheating of the thruster structures. The reason for the action of the third mechanism is the knocking out of atoms of the surface layer of elements of the electrode system as a result of bombardment by plasma ions, ionization and capture of knocked out atoms by the plasma flow and their removal beyond the discharge gap. The action of the third destruction mechanism is characteristic of ion-plasma thrusters in the acceleration zone of which the plasma is not in a quasi-neutral state.

The energy that feeds the described destruction mechanisms is the energy losses in an electric rocket thruster.

The advantages of Electric Propulsion Thrusters over chemical rocket engines include:

- EPT resource can be hundreds of times greater than the resource of chemical rocket engines;
- the specific impulse of modern EPT is tens of times greater than the specific impulse of chemical engines;
- separation of the energy source and the working fluid in the EPT allows overcoming the restriction inherent in chemical engines – a relatively low flow rate and the need in great amount of oxidizer and propellant.

The main operational requirement of a promising spacecraft is the creation of a sufficiently powerful EPT, but so far there is no such thruster – the most powerful commercially available EPT models have a thrust in the range of 0.05–0.10 N, and experimental thrusters with a specific impulse of the order of 10^5 s have a thrust in the range of millinewtons. The world experience in creating experimental high-power EPTs shows that there are two main problems in their wide development and implementation:

1) the problem of creating an onboard electric power source for a high-power spacecraft; this issue is beyond the scope of this research;
2) the destruction of powerful EPT structures.

The problem of EPT power limitation due to thermal destruction can be solved using an efficient cooling system of thruster structural elements, including modern high-temperature superconducting magnets that can be used to form the magnetic field necessary for an EPT to operate. The proposed research is dedicated to the solution of this problem. For that, it is necessary first of all to analyze the features of mechanisms of energy conversion in EPT.

2. ENERGY CONVERSION MECHANISMS IN EPT ANALYSES

An electric propulsion thruster is a converter of electrical energy into kinetic energy of a plasma stream. In plasmatron (electro thermal) thrusters, as well as in classic chemical rocket engines, it is expressed as mechanically directed movement of a jet stream heated either by a current passing or by an arc discharge (as an exothermic chemical reaction) to the state of a low-temperature plasma of the working fluid. The plasma in such EPTs is neutral and consists of randomly moving (thermal motion) constantly recombining and dissociating ions, essentially being a plasma only until a sufficient amount of energy is scattered so that the temperature of the recombined pair of ions is lower than the ionization energy and the working fluid goes back into a molecular state.

In electrostatic and electromagnetic thrusters, the kinetic energy of the plasma stream is the sum of the kinetic energies of the ions of the working fluid, accelerated by exposure to electric and magnetic fields. The mass of positive and negative ions of the working fluid differs by at least three orders of magnitude, that is why usually the positive ions of the working fluid need to be accelerated, to do this they need be pre-ionized.

It should be noted that the use of the mechanism of acceleration of positive ions leads to the separation of quasi neutral plasma – positive ions mainly flow out of the thruster, and the movement of plasma electrons ends with their capture by a shielding electrode or a magnetic trap field. Thus, when the thruster is operating, an ever-increasing electric charge arises, and, consequently, the potential of the thruster and the spacecraft constantly increases (the EPT action resembles a Van de Graaff generator). This, in addition to the danger of destruction of electrical systems due to the effects of a spark discharge, leads to the appearance of Coulomb forces acting on the spacecraft and changing its orbit, as well as attracting neutral space objects to it (for example, micrometeorites or space debris).

Processes in electrothermal thrusters are fairly simple – they are quite similar to processes in chemical thrusters, including the processes of overheating and thermal destruction. For this reason, the approach for cooling systems calculation, design and development, proposed in the Thesis is easily applicable to electrothermal thrusters. That is why in this Thesis the will not focus only on electrothermal thrusters only, but pay attention also to electrostatic and electromagnetic thrusters.

To understand the nature of the energy conversion loss in the electrostatic and electromagnetic thrusters, it is necessary to consider the possible mechanisms for accelerating the ions of the working fluid, i.e., the mechanisms of formation of accelerating forces.

The analysis showed that the main forces action of which is used in various models of ion-plasma thrusters to accelerate the ions of the working fluid are as follows.

The Coulomb force, which imparts to the ion the acceleration from the action of the electric (electrostatic) field equal to the product of ion charge q_i and the electric field strength $\boldsymbol{E}$, hereinafter the vector quantities indicated in bold.

The effect of the Coulomb force is the main accelerating factor in electrostatic thrusters, but it is also used in some electromagnetic thruster classes: Gridded Ion Engine (GIE), Hall

Effect Thruster (HET), High Efficiency Multistage Plasma Thruster (HEMPT), Pulsed Plasma Thruster (PPT), Quad Confinement Thruster (QCT) and some of Electrode-less Thrusters.

The Lorentz force, which imparts to the ion acceleration due to the magnetic field, equal to the product of the ion charge by the vector product of the ion velocity and magnetic field induction: $q_i(\boldsymbol{v}_i \times \boldsymbol{B})$. Hereinafter, × is the sign of the vector product.

Using the Lorentz force, thrusters can be built based on ion-cyclotron and electron-cyclotron resonances, development of which is currently underway. Similar EPTs are classified by EPIC as Electrode-less thrusters [8].

The Lorentz force is widely used to translate electron trajectories in the ionization chamber from linear to closed orbits, which makes it possible to increase the probability of electron impact on the neutral atom of the working fluid and, therefore increase the degree of ionization of the working fluid. Magnetic systems that create, together with an electrode system of this kind, the effect of the Lorentz force are used in many types of modern EPTs, for example, in the Hall- Effect Thruster (HET) [8].

The force is obtained because of the current flow through the plasma due to collision of an ion with a directed stream of plasma electrons. Acceleration due to the action of this force is called Ohmic acceleration or acceleration of the "electronic wind".

In a hydrodynamic plasma model, the "electron wind" effect is equal to the ratio of the product of the ion charge and current density to plasma conductivity $\frac{q_i J}{\sigma}$ [9].

This force (combined with the Lorentz force) is used to accelerate ions in Magneto Plasma Dynamic (MPD) thrusters.

The force of gas-dynamic or thermal acceleration arising due to the ion pressure gradient, due to which the chaotic thermal movement of ions becomes directed, and the randomly directed forces of thermal collisions form a directed resultant vector. It can be said that the action of this force is of an auxiliary character, since the achievement by this force of the values that affect the ion acceleration is a characteristic only of certain types of Magneto Plasma Dynamic (MPD) thrusters [8].

In hydrodynamic plasma model, this force is approximately equal to the ratio of the ion pressure gradient to the plasma concentration $\frac{\nabla P_i}{n}$ [9].

The process of creating reactive thrust in electrostatic and electromagnetic thrusters is due to the acceleration of charged particles – positive ions of the electrostatic and electromagnetic thruster's working fluid, so the speeds of neutral atoms and plasma ions of the working fluid differ by several orders of magnitude.

Neutral (non-ionized) atoms of the working fluid practically do not participate in the creation of the thrust and reactive power of electrostatic and electromagnetic thrusters. Because the velocities of the accelerated ions outflow exceed the velocities of neutral atoms by several orders of magnitude, they determine the velocity of the outflow of working fluid of the thruster v_{eq}. In this case, the mass flow rate of the accelerated working fluid G will be the mass flow rate of ions G_i equal to the product of the number of ions n_i and the mass of the working fluid ion m_i.

Then thrust T expression for electrostatic and electromagnetic thrusters takes the following form:

$$T = -v_{\text{exi}}(m_{\text{i}}\, n_{\text{i}}), \tag{2.1}$$

where v_{exi} is exhausting velocity of accelerated ions.

Specific impulse I_{sp} of electrostatic and electromagnetic thrusters can be defined as:

$$I_{\text{sp}} = \frac{v_{\text{exi}}}{g}. \tag{2.2}$$

In general, the equation of ion motion in an electromagnetic field under conditions of a rarefied plasma is as follows [4]:

$$m_{\text{i}} \frac{\mathrm{d}v_{\text{i}}}{\mathrm{d}t} = q_{\text{i}} \times \boldsymbol{E} - \frac{\nabla P_{\text{i}}}{n} - \frac{qj}{\sigma} + q_{\text{i}} \left(\boldsymbol{v}_{\text{i}} \times \boldsymbol{B}\right). \tag{2.3}$$

There are two types of ion acceleration in an electrostatic field:

- acceleration of ions actually in an electrostatic field;
- ion acceleration due to the combined action of electric and magnetic fields.

In the first case, the component of the EPT traction force generated by the electrostatic field is formed as the mechanical reaction force of the electrodes to the resulting Coulomb force, which arises as a result of interaction of the working fluid ions and the electric field of electrodes with different potentials. This pure acceleration mechanism is used in electrostatic EPTs of the Gridded Ion Engine (GIE) type [8].

In the second case, with the combined action of electric and magnetic fields, the Hall-effect manifests itself – in a conducting plasma through which current flows, a bias current arises, which significantly changes the acceleration mechanism compared to an electrostatic thruster.

A schematic diagram of an EPT with cross electric and magnetic fields – Hall-Effect Thruster (HET) [8], illustrating the effect of an electric and magnetic field on an ion, is shown in Fig. 2.1.

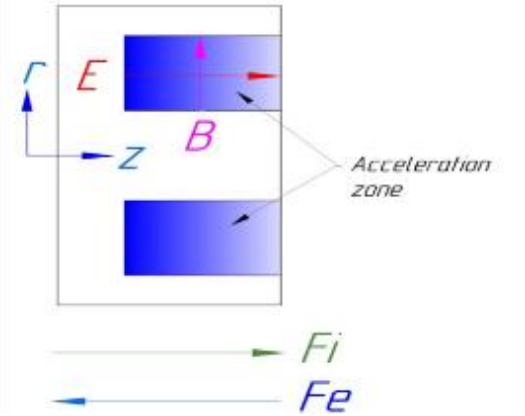

Fig. 2.1. Schematic diagram of EPT with cross electric and magnetic fields.

In EPT with acceleration of ions in crossed electric and magnetic fields, the traction force increases due to the additional action of the Ampere force on the ion flux [10].

3. EPT THERMAL BALANCE CONCEPT AND ITS ESTIMATION

EPT Thermal balance concept

Thermal power supplied to EPT structure can be determined by subtracting from the total amount of thermal power Q_t released during EPT operation (EPT emitted thermal power) the amount of thermal power allocated outside EPT with the working fluid flow Q_{wf}. Since there are mechanical connections between the elements of EPT structure inside the thruster and the distance between them is relatively small, it means that the main mechanism of heat transfer in EPT structure is thermal conductivity. From the other side outer space vacuum around EPT is a highly efficient heat insulator. The processes of convection and heat conduction in outer space are absent. The only heat transfer mechanism is radiation, and the thermal energy absorbed by EPT can be removed outside the thermodynamic system of EPT only by radiation: a heated EPT is a source of thermal radiation, and power Q_r radiated by EPT is subtracted from the absorbed one.

The difference between the absorbed and radiated thermal power determines the condition of EPT thermal balance:

$$Q_t - Q_{wf} = Q_r. \tag{3.1}$$

In addition, with an increase of EPT power its heat balance shifts toward an increase in radiated power and, consequently, in the temperature of the thruster structure, since the radiation surfaces of EPT cannot dissipate the supplied heat. EPT starts to overheat – the equilibrium temperature may be outside the operation range of EPT materials (cable insulation, magnet's Curie point, etc.) and to prevent the overheating of EPT, it is necessary to embed a thermal throttle into its control system, i.e., special controlled valve. It means to artificially reduce thrust, specific impulse and power to prevent overheating, and thruster failure. Such a need arises even for EPT with a consumed electric power of 660 W (thruster *SPD-70*) [11].

An alternative to artificial decreasing of EPT performance is to create an EPT cooling system that allows excess heat output to be removed outside EPT and then dissipating it in outer space.

EPT emitted thermal power

EPT is a converter of electrical energy into kinetic energy of plasma stream. One of the main characteristics of EPT is the kinetic power of the working fluid, also called reactive power, P_{jet}:

$$P_{jet} = \frac{1}{2} G V_{exi}^2, \tag{3.2}$$

where G is the working fluid mass flow and V_{exi} is the working fluid exhaust velocity.

Kinetic power can also be expressed through EPT thrust T and its specific impulse I_{sp}:

$$P_{jet} = \frac{1}{2} T I_{sp} g. \tag{3.3}$$

For EPT the ratio of the effective power, i.e., its reactive power P_{jet}, to electric power P consumed by EPT is EPT's total efficiency η:

$$\eta = \frac{P_{jet}}{P}. \tag{3.4}$$

Losses of energy conversion, per second, into electric propulsion power is EPT power loss P_L:

$$P_L = (1 - \eta)P \text{ or } P_L = P - P_{jet}. \tag{3.5}$$

In theory, all losses of energy conversion in EPT can be represented as heat loss: in current conductors, plasma heat transfers to EPT structure, losses for heating of chaotically moving neutral atoms of plasma flow, then as divergence of ion beam (value of which is less than 10 % and can be minimized as will be described further) and as electro-erosive destruction of EPT structures.

Thus, it is proposed to be guided by the assumption that the heat power released during the operation of EPT is the total power loss of the conversion of electric energy into kinetic energy of the ion beam P_L. The difference between P_L and Q_t is only the parasitic power of the part of the diverging ion flow, which does not fall on EPT structure, but whose trajectory is not strictly opposite to EPT thrust vector.

Reduction of EPT thermal power by working fluid flow

The following approach is proposed to assess the thermal power diverted outside the thruster by the flow of the working fluid. The heat power diverted by the flow of the working fluid into the outer space is equal to the rate of change of the thermal energy of the working fluid mass, and for the discrete mass of the working fluid, emitted by EPT per unit time, it can be determined as

$$Q_{wf} = C_{wf} G \Delta T_{wf}, \tag{3.6}$$

where C_{wf} is the specific heat of the working fluid in J/(kg K), ΔT_{wf} is change in the average temperature of the working fluid when passing through EPT, K, which is almost equal to outgoing plasma temperature. In the stationary mode of EPT operation, it is about specific heat, as specific heat capacity at constant pressure is C_p.

According to [12], C_p of plasma is the combination of translational $C_p(T)$, rotational $C_p(R)$, vibrational $C_p(V)$, and electronics $C_p(E)$ energy modes. It is defined by expression

$$C_p(T) = C_p(T) + C_p(R) + C_p(V) + C_p(E). \tag{3.7}$$

Calculation of thermal regime for the EPT should be guided by a value close to the minimum of the thermal power diverted by the flow of the working fluid – 0.7 % of the electric power supplied to the EPT. In this case, the error is equivalent to a decrease in the

actual heat load on the cooling system compared to the calculated one, i.e., it has some power reserve (max. 9 %).

From the above, it follows that there is a significant difference between chemical thrusters and EPTs. It lies in differences of self-cooling mechanisms. In a chemical thruster, heat removal from structural elements is effectively carried out due to heat removal by mass flow of the working fluid with the great mass flow rate (kg/s) and it is sufficiently effective. Whereas in EPT, due to the small mass flow rate in it (mg/s), cooling due to heat removal by the working fluid is not effective and removes no more than 10 % of the generated heat.

Assessment of the need to create a cooling system for EPT

The criterion for the need to create a cooling system for EPT is the risk of overheating. In this regard, at the initial stage of its development (when the basic characteristics of the electrode and magneto-optical systems are determined), it is necessary to assess the danger of possible overheating of structures.

The following method is proposed for a preliminary assessment of EPT overheating, that is, the need to create a cooling system and determine the maximum thermal load power based on the following factors:

- according to the thrust and specific impulse of the thruster reactive power P_{jet} is determined;
- based on the calculated or experimentally obtained value of electric power, the total EPT efficiency is determined and the total power loss P_L is determined;
- the value of heat power Q_{wf}, diverted by the working fluid flow into the outer space, is determined, or this value is equal to 0.7 % of the EPT electric power;
- the maximum value of thermal power Q_t is equal to P_L;
- from the thermal balance equation, power Q_r radiated by EPT is determined;
- based on the obtained value of Q_r and on the geometric and structural characteristics of the thruster, average temperature of EPT structure is determined.

If the obtained average temperature value is outside the operational range of any elements of the electric propulsion system, then **there is a need to create a cooling system for this EPT**. **As a rule, for an EPT with an electric power of more than 1.5 kW, either artificial limitation of EPT power with decreasing temperature or a cooling system device is necessary.** Since the power-limited option is not an acceptable solution, there is a need to create an EPT cooling system.

Description of EPT thrust processes

The velocities of neutral atoms and ions in EPT output plasma differ by several orders. Consequently, neutral atoms play practically no role in creating EPT thrust. Taking into consideration that the EPT working fluid consists of particles and that EPT thrust T is determined by the outflow velocity V_{exi} of accelerated ions and their mass flow rate G_i, equal to product of ion mass m_i and its flow n_i (number of ions per second), it is possible to obtain the following expression:

$$T = -V_{exi}(m_i n_i). \tag{3.8}$$

The kinetic power of the particle beam is expressed as

$$P_{jet} = \frac{T^2}{2m_i n_i}. \tag{3.9}$$

It means that **to increase the thrust without increasing the mass flow rate it is necessary to increase the reactive power of the thruster**.

The energy of electrostatic field E, which accelerates the working fluid ions, is equal to the product of the working fluid ion charge q_i and the potential difference V_b of the electric field of thruster accelerator. After conversion to the kinetic energy of the ion, in accordance with the law of energy conservation, it is equal to the kinetic energy of the ion:

$$E = V_b q_i = \frac{1}{2} m_i v_{exi}^2. \tag{3.10}$$

From (3.10), the ion flow velocity is expressed as

$$V_{exi} = \sqrt{\frac{2V_b q_i}{m_i}}. \tag{3.11}$$

The ion beam current I_b is equal to the product of the ion charge q_i and the number of ions n_i, which can be expressed through the mass flow of ions G_i:

$$I_b = \frac{q_i G_i}{m_i}. \tag{3.12}$$

It means that the mass flow of ions can be expressed via ion beam current:

$$G_i = \frac{I_b m_i}{q_i}. \tag{3.13}$$

From expression (3.8), by substituting into it the variables expressed from Equations (3.11) and (3.13), taking into account that the ions in EPT have mostly a single unit degree of ionization, which means that the unit charge is equal to the elementary charge e, the following expression is obtained for EPT ideal thrust (in Newtons):

$$T = \sqrt{\frac{2m_i}{e}} \cdot I_b \sqrt{V_b}. \tag{3.14}$$

This form is convenient in that the first factor of Expression (3.14) is a constant for each type of working fluid.

Evaluation of the EPT efficiency

Due to (3.14) an ideal EPT specific impulse is

$$I_{sp} = \frac{V_{exi} G_i}{gG}. \tag{3.15}$$

The ratio of the ion mass flow per second to the mass flow per second of the working fluid, called the **index of the efficiency of the working fluid mass flow usage η_m,** in the case of a singly charged ion flow can be defined using the following expression:

$$\eta_m = \frac{I_b m_i}{eG}. \tag{3.16}$$

For a real EPT, taking into account all real thruster effects described before, with allowance for the correction coefficient γ, the expression for the mass utilization efficiency index is

$$I_{sp} = \frac{\gamma \eta_m}{g} \sqrt{\frac{2eV_b}{m_i}}. \tag{3.17}$$

Substituting in (3.16) all the determined values, we obtain the value of the single conversion factor (in SI units):

$$I_{sp} = 1416.5288 \gamma \eta_m \sqrt{\frac{V_b}{M_a}}, \tag{3.18}$$

where M_a is the mass of the working fluid ion in atomic mass units.

Thus, the rate of exhaust velocity (and, correspondingly, for specific impulse) increases with a decrease in the atomic mass of the working fluid.

The overall efficiency η is the ratio of reactive power P_{jet} to electric power P:

$$\eta = \frac{T^2}{2GP}. \tag{3.19}$$

All the needs for (3.19) parameters can be determined and measured during EPT tests (thrust, mass flow and electrical power consumption). Therefore, (3.19) is important for the design and development of EPT because overall efficiency of EPT can be determined experimentally.

4. DEVELOPMENT OF A MATHEMATICAL MODEL OF EPT COOLING SYSTEM

Physical principles and approaches are presented to design mathematical models of EPT cooling systems, determine the thermal regimes of its elements, and thereby achieve long-term and reliable operation. A mathematical model developed on the basis of the heat balance equation and the structural diagram of the EPT cooling system includes 3 elements: a heat-receiving subsystem, heat transfer subsystem, and heat dissipation subsystem. When developing the mathematical model, the method of step-by-step problem solving is used. The following steps are to be followed.

1. Statement of the problem, formulation of initial data and boundary conditions.
2. Modeling of processes occurring in the heat-receiving subsystem of EPT.
3. Development of a calculation model of the heat-receiving subsystem of EPT.
4. Determination of the type of refrigerant used in the system.
5. Development of a method for hydraulic calculation of the EPT cooling system.
6. Modeling of the heat dissipation subsystem.

Statement of the problem and initial data

The initial data for mathematical modeling of the cooling system are: the value of thermal power of the cooling system load Q_{in}, determined according to the methodology, proposed in the previous section; geometric characteristics of the electrode system; specification of prospective materials for the electrode system (data on their physical characteristics).

These data are obtained as a result of experimental studies of a prototype developed by the author of the electric propulsion system, taking into account corrections for scaling.

Modeling of processes occurring in the heat-receiving subsystem of the EPT

The heat-receiving subsystem is a set of thermal bridges and pipelines through which the refrigerant moves, arranged in the body of the electrodes and other structural elements to collect and remove excess heat power output beyond the EPT. The diagram is shown in Fig. 4.1.

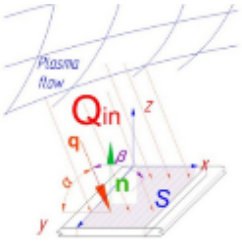

Fig. 4.1. Generalized diagram of EPT for heat process calculation.

The heat conduction process in general is described by Maxwell–Cattaneo law [56]:

$$\boldsymbol{q} + \tau \frac{\partial \boldsymbol{q}}{\partial t} = -k(\theta)\nabla \boldsymbol{T}, \tag{4.1}$$

where $\boldsymbol{q}$ is the vector of a local heat flux density, W/m^2; τ is the system relaxation time, s; $\partial\boldsymbol{q}/\partial t$ is the differencial of a local flux density vector over time; $k(\theta)$ is the material's thermal conductivity, as a function of temperature, W/(m K); $\nabla\boldsymbol{T}$ is the vector of a temperature gradient, K/m.

This equation takes into account the dynamic properties of the thermal system, that is, the presence of a temporary shift between the change in the heat flux incident on the heat-receiving surface and the change in its temperature, and it can be reduced to the next differential equation:

$$-\tau\frac{\partial \boldsymbol{q}}{\partial t}+k(\theta)\left(\frac{\partial\theta}{\partial x}\times\vec{e}_x+\frac{\partial\theta}{\partial y}\times\vec{e}_y+\frac{\partial\theta}{\partial z}\times\vec{e}_z\right)-\boldsymbol{q}=0. \tag{4.2}$$

After transformations, Equation (4.2) takes the following form:

$$-\tau\frac{\partial}{\partial t}\left(\frac{\mathrm{d}Q_{\text{in}}}{\mathrm{d}A_{\text{h}}}\sin\alpha\sin\beta\right)+k(\theta)\left(\frac{\partial\theta}{\partial x}\times\vec{e}_x+\frac{\partial\theta}{\partial y}\times\vec{e}_y+\frac{\partial\theta}{\partial z}\times\vec{e}_z\right)-\frac{\mathrm{d}Q_{\text{in}}}{\mathrm{d}S}\sin\alpha\sin\beta=0. \tag{4.3}$$

Equation (4.3) is a general heat equation. By integrating Equation (4.3) over the area or coordinates and time, it is possible to obtain data on the distribution of the temperature field over the heat-absorbing surface in real time.

The author used a special case of the formulation and solution of equation (4.3) corresponding to the problem of finding the heat-absorbing surface temperature distribution, which does not require experimental data at the initial stage, but gives a satisfactory practical result.

This method is based on the refinement of boundary conditions as applied to the specific problem of the temperature distribution in the heat-receiving subsystem of the EPT cooling system. Thus heat-receiving subsystem is designed so that the heat-receiving surface transfers heat to the refrigerant, which is moving in pipes and through the thruster structure heat bridges, thus the calculation model can be refined and simplified. The entire heat-receiving subsystem should be divided into elementary cooling cells C_1–C_i, consisting of sections of the heat-receiving surface connected by thermal bridges to sections of the refrigerant pipes, that is, the cells that consist of elementary pipes filled with refrigerant that is circulating through the cooling system, Fig. 4.2.

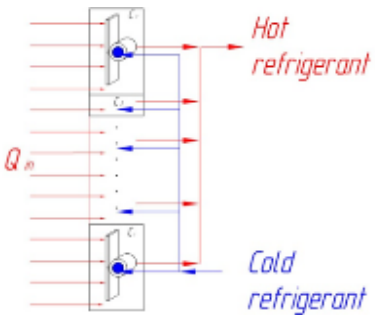

Fig. 4.2. Diagram of the heat receiving subsystem of EPT cooling system.

Thermal power Q_{in} that is absorbed by the thruster's entire heat-receiving surface is the thermal load of the thruster cooling system, and this thermal power is supplied to and absorbed by the entirety of the heat-receiving surfaces of all elementary cooling cells C_1–C_i. A cold refrigerant with temperature T_1, enters the elementary pipe and, after heating to temperature T_2 and by the heat transferred from the heat-receiving surface, exits from the elementary pipe. The diagram of a model of the heat-receiving subsystem neighboring cells C_{i-1}–C_i is presented in Fig. 4.3.

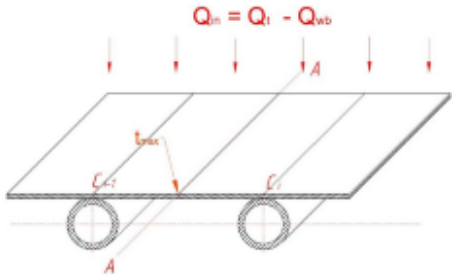

Fig. 4.3. Diagram of the heat receiving subsystem cells.

The boundary A–A between cells is arbitrary, and its position is determined from a subsequent calculation of the cell geometry, as the midpoint of the distance between the pipes with refrigerant, which, in turn, is determined as the maximum distance between the pipes. This distance meets the criterion of sufficiency of the heat power selection, which incident on the heat-receiving surface, at geometrical and hydraulic characteristics of the cell. **An indicator of the sufficiency of the thermal power removal is the calculated temperature of the heat-receiving surface of the cell**, the maximum value of which, T_{max}, is achieved on the surface, on the cells' boundary line A–A.

The indicated maximum temperature should be within the limits specified in the initial data, which is determined based on the strength and stiffness conditions of the EPT materials, characteristics of magnets, characteristics of combustion stability of a gas discharge, etc. The distance between the pipes should be the maximum possible based on the conditions of reducing material consumption and complexity of EPT manufacturing.

Development of calculation model

The model of the heat receiving surface of EPT structure is shown in Fig. 4.4.

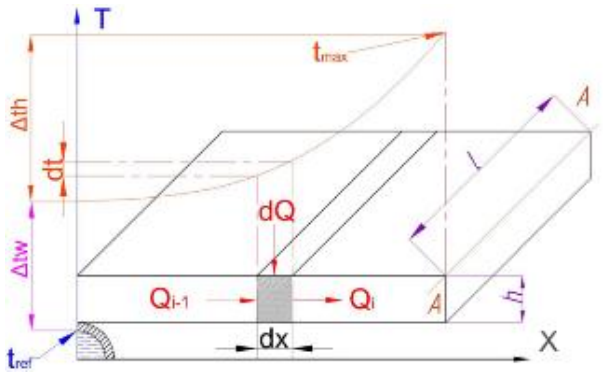

Fig. 4.4. Thermal surface model.

The following coordinate system is chosen for developing a mathematical model:

- the *X* axis of the coordinate system is parallel to the heat-receiving surface and perpendicular to the pipe and line *A*–*A*;
- the *Y* axis is perpendicular to the *X* axis, crosses it and is located in the plane of the heat-receiving surface (aligned with the pipe axis and line *A*–*A*);
- the *Z* axis is normal to the heat-receiving surface and is crossing the pipe axis.

Distance *l* is such that the contact line of the pipe containing the refrigerant and the heat-receiving surface can be represented as an isothermal line. Due to greater efficiency of the heat conduction mechanism of the heat-receiving surface in comparison with the radiation mechanism of supplying thermal power Q_{in} to it, with this choice of the coordinate system, isotherms on the heat-receiving surface are parallel to the pipe axis and, accordingly, there is no temperature gradient along the *Y* axis. The thickness of the material of the heat-receiving surface *h* is sufficiently small compared to its length and width. Under the condition of good thermal conductivity of the material over the thickness, it warms up completely and evenly, there is no temperature gradient over the thickness of the material (i.e., along the *Z* axis). Thus, **in the proposed calculation model, the temperature gradient is available only along the *X* axis**, and the vector of the temperature gradient is parallel to the *X* axis.

The processes in EPT are quasistatic because usually EPT works with equal thrust and discharge parameters for a long time. Therefore, to build a mathematical model, it is enough to use the static form of Maxwell–Cattaneo law and Fourier law:

$$\boldsymbol{q} = -k\,\nabla \boldsymbol{T}. \tag{4.4}$$

In the proposed coordinate system, the temperature has a gradient in only one direction – along the *x* coordinate, therefore, the nabla operator for temperature degenerates into a differential along the *x* coordinate:

$$\boldsymbol{q} = -k\frac{\mathrm{d}t}{\mathrm{d}x}. \tag{4.5}$$

On the heat-absorbing surface an elementary segment of length d*x* is selected. The temperature change in segment d*x* will be equal to d*t*. The heat balance equation for the region bounded by d*x* will have the following form:

$$Q_i - Q_{i-1} = \mathrm{d}Q. \tag{4.6}$$

In practical EPT constructions, the electrode system is either a set of cylinders, or one of the electrodes has the shape of a slightly expanding cone. Therefore, and after some transformations of the equations, **obtain the equation, describing the thermal field on heat receiving surface**:

$$\frac{\mathrm{d}^2 t}{\mathrm{d}x^2} + \frac{\boldsymbol{q}}{kh} = 0. \tag{4.7}$$

The solution of Equation (4.7) is the following function *T*(*x*), which describes the temperature distribution along the length of the heat-absorbing surface (axis *x*):

$$T(x) = -\frac{q}{2kh}x^2 + k_1 x + k_2. \tag{4.8}$$

To facilitate finding, the coefficients, when solving this equation, combine the models shown in Figs. 4.3 and 4.4 are compatible. If the distance between adjacent thermal bridges, between the pipe and the heat-receiving surface along the *X* axis, is designated as *D*, then the *x* coordinate value corresponding to the position of the T_{max} line will be *D*/2. Then the vertex of parabola *T*(*x*) corresponding to Function (4.8), i.e., the point of the max. temperature of the heat-absorbing surface will be on the axis perpendicular to the *X* axis and passing through the point *x* = *D*/2, Fig. 4.5.

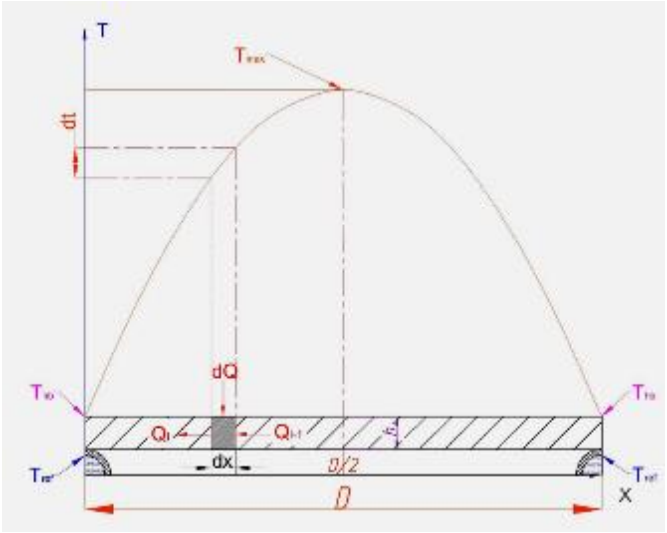

Fig. 4.5. Complete heat transfer surface model.

Coefficient k_2 of Equation (4.8) will be equal to the minimum temperature of the heat-absorbing surface in cross-section *D*, i.e., the temperature of the thermal bridge between the refrigerant pipe and the heat-receiving surface T_{hb}. Coefficient k_1 of Equation (4.8) is determined as follows. On the one hand, the *x*-axis coordinate of the parabola is k_1 divided by $2\left(-\frac{q}{2kh}\right)$, and on the other hand, it is equal to *D*/2. Then:

$$k_1 = \frac{Dq}{2kh}. \tag{4.9}$$

Thus, the solution of Equation (4.7) has the following form:

$$T(x) = -\frac{q}{2kh}x^2 + \frac{Dq}{2kh}x + T_{hb}. \tag{4.10}$$

The maximum temperature isotherm has the form of a straight line located on a heat-absorbing surface parallel to the refrigerant pipes and passing through the point with *t* coordinate *x* = *D*/2.

Thus, the maximum temperature of the heat-absorbing surface T_{max} will be

$$T(x) = -\frac{q}{2kh}x^2 + \frac{Dq}{2kh}x + T_{hb}. \quad (4.10)$$

$$T_{max} = \frac{q}{8kh}D^2 + T_{hb}. \quad (4.11)$$

Based on a detailed mathematical analysis of the ways to solve this equation, it has been ascertained that with equal heat flux density acting on the heat-absorbing surface and the specified properties of the refrigerant materials and the surface and tube material, **the main factors determining the maximum premised operating temperature are the distance between the pipes and the velocity of movement of the refrigerant**.

Determining the refrigerant type used in the cooling system. The type of refrigerant is determined primarily based on the required temperature range and thermodynamic characteristics of the refrigerant (high specific heat and thermal conductivity, low density and, in some cases, low dynamic viscosity). The best refrigerants are liquid metals with a relatively low melting point (mercury, tin, lead, sodium, potassium, lithium), but they have significant specifics of application, primarily the operating temperature range, toxicity, current conductivity and chemical activity. Good refrigerants are water, aqueous solutions and substances that are in a liquid state under normal conditions (i.e., ammonia solution, ethylene glycol). The worst refrigerants are cryogenic liquids (liquid nitrogen, liquid argon, liquid xenon and liquid helium). They have a relatively low heat capacity and thermal conductivity, as well as low density. The determining condition for the use of cryogenic liquids is the required cryogenic temperature range of the cooled object, for example usage of high temperature superconductor magnets in thruster accelerator.

Hydraulic calculation of the EPT cooling system

The next step in the mathematical simulation process is the hydraulic calculation of the EPT cooling system. First of all, the required total volumetric and mass flow rate of the refrigerant through all the cells of the heat-receiving subsystem have to be determined.

Since all the thermal energy absorbed by the heat-receiving subsystem should be used to heat the refrigerant, the required volumetric flow rate of the refrigerant is determined based on the permissible increase in the temperature of the refrigerant supplied to the heat-receiving subsystem during its heating until ΔT_{ref}:

$$\Delta T_{ref} = T_{refout} - T_{refin}, \quad (4.12)$$

where T_{refin} is the temperature of the refrigerant entering the heat-receiving subsystem, K; T_{refout} is temperature of the refrigerant leaving the heat-receiving subsystem, K.

When determining ΔT_{ref}, it is necessary to take into account and evaluate the possibility of further heating of the refrigerant when passing through pipelines in the heat transfer subsystem and the heat dissipation subsystem, as well as in the pump of the heat transfer subsystem, and reduce the maximum value of ΔT_{ref} by the possible reached heating temperature.

Heat dissipation subsystem

The task of the heat dissipation subsystem is the removal of thermal energy from the refrigerant and the dissipation of this energy to outer space. This task is performed by radiators – heat exchanging surfaces of a large area located on the shadow side of the spacecraft. As a rule, such radiators are equipped with reflectors or "blankets" of screen-vacuum thermal insulation that prevent irradiation from other spacecraft's structures, as well protect from the Sun and the Earth heat radiation and provide radiator's heat radiation in a given direction. This, however, should not affect the thermal mode of other functional space equipment apparatus. It should be noted that such radiators are a unified structural element of spacecraft, since they are used in spacecraft thermal control systems. Therefore, the best way will be the selection of a commercially available radiator based on the characteristics obtained during the proposed model calculation: power to dissipation, inlet and outlet refrigerant temperatures, and its pressure and flow rate.

The heat dissipated by the refrigerant through its radiation into outer space

In this case, heat from the liquid is initially taken to the walls of the pipes and through those walls transferred to the edges of the heat-emitting surface (radiator). The initial data for its calculation are the known values of pressure P_{ref}, the mass and volume flow rates G_{ref} and σ_{ref}, as well as the amount of excess heat power that should be removed from the system – the radiation power Q_r.

5. CALCULATION METHOD, CALCULATION ALGORITHM AND COMPUTER CALCULATION PROGRAM FOR EPT COOLING SYSTEM

Based on the described physical and mathematical model, a calculation procedure was developed, and on its basis, a calculation algorithm and software for the calculation of the mathematical model parameters of the EPT cooling system. Here also was used the method of step-by-step problem solving.

Source data collection

The source data are: the value of the thermal power of the cooling system load Q_{in} determined according to the procedure proposed in Section 3 of this Thesis; characteristics of the electrode system; specification of prospective materials for the construction of the electrode system (data on their physical properties). These data can also be obtained as a result of experimental studies of the EPT prototype being developed, taking into account corrections for scaling obtained using similarity methods (scaling laws), as, for example, it was proposed for Hall-effect thrusters in [55]. It seems very likely, that analogous similarity laws can be obtained for other types of EPT. Selection of materials for the heat-absorbing surface and pipes, selection of the refrigerant, determination of the necessary characteristics based on the specification or on the basis of design requirements, the structural material is determined that can be applied to produce the heat-absorbing surface and pipes for the refrigerant. The necessary and permissible operating temperature range of this material is determined according to the conditions of strength and stiffness. T_d is determined as the maximum allowable temperature of the heat-absorbing surface of the heat-receiving subsystem. Based on a given range of operating temperatures, the type of refrigerant is determined by the following criteria: the content of the liquid phase is maximal, and the vapor content is minimal. Then chosen refrigerant, which having the maximum: a) thermal conductivity, b) density, c) heat capacity (factors in decreasing order of importance), finally the refrigerant with the lowest dynamic viscosity is selected, also fire and explosion hazard, current conductivity, toxicity, availability and cost are taken into account.

A table is compiled of thermal conductivity of the structural materials in the range of operating temperatures and beyond with tolerance ±20 % of the upper and lower boundaries of this range.

Analysis of the design and determination of the initial structural data

Analysis of the thruster design is performed. The geometry of the heat-receiving surface is determined. Based on the geometric characteristics of heat-absorbing surfaces, the total area of heat-absorbing surface A_h is determined.

Calculation of the characteristics of the cell heat receiving subsystem

Using the method of successive approximation – by sequential calculations define the heat-absorbing surface, then determine the thickness of the material, the structurally and technologically permissible width and height of thermal bridges, the geometric characteristics of the pipes for the refrigerant and the distance between the pipes of refrigerant. In mathematical modeling of variation, the following characteristics of the heat-receiving subsystem, i.e., variables, arranged in increasing order of the structural and technological complexity, are subject of the change, varying step-by-step within structurally defined limits. This is the distance between the pipes D, it varies in the direction of decrease with a step of 0.1 mm from the initially specified structurally determined maximum value D_0 to the minimum structurally possible value D_{min}. Then the velocity of the refrigerant movement in the pipes V_{ref} varies in the direction of increase from the initially set value of V_{ref0} in increments of 0.001 m/s to V_{refmax}, determined based on the design characteristics of the pumps that can be used in this range. In addition, the thickness of the heat-absorbing surface h – initially varies in the direction of increase with a step of 0.1 mm from the initially structurally determined h_0, see (4.11), to the maximum structurally permissible value h_{max}. If, as a result of the calculation, the relation $T_{max} \leq T_d$ worsens (where T_d is the predetermined structure temperature), i.e., the value of T_{max} increases, the parameter varies in increments of 0.1 mm downward. It means that the initial temperature of the refrigerant T_{ref} varies in the direction of decreasing from value T_{ref0} with a step of 0.1 K to value T_{refmin}, determined based on the characteristics of the refrigerant and the maximum possible radiator area of the heat dissipation system. The results of the variation of this parameter subsequently affect the determination of the area of the radiator of the heat dissipation system, i.e., the last variable is the inner diameter of the refrigerant pipes d in the direction of increase in increments of 0.5 mm. If the diameter of the pipes was changed during the calculation, it is necessary to verify the preservation of the conditions of strength and stiffness of the walls of the pipes at a given pipe wall thickness z. As well as check the technological possibilities of maintaining (or the necessity to increase) the contact spot of the pipe with the heat-absorbing surface.

Hydraulic calculation of cooling system

Hydraulic calculation of pipes of the heat-absorbing surface, pipelines of the cooling system and the pump is carried out in accordance with the aforementioned order. Based on the analysis of the principle hydraulic circuit and the installation diagram of the cooling system, a table of local resistances is compiled and the corresponding similarity coefficients are determined. A table of pipelines is compiled in which the velocities of the refrigerant in different cross-sections of the pipelines are determined, as well as the corresponding similarity numbers. Loss of elements, total losses and total head (pressure) of the cooling system pump are determined.

Selection or calculation of the heat dissipation subsystem

If it is possible to choose from a number of commercially available spacecraft thermal control systems based on the obtained data of the required dissipation power, temperatures of the incoming and outgoing refrigerant, pressure and flow rate of the refrigerant, the most suitable radiator be selected. If this is not possible, the radiator elements of the heat dissipation subsystem are calculated.

Thus, all the necessary characteristics of the structural elements of the cooling system are uniquely determined. Based on the proposed methodology, an algorithm for calculating the EPT cooling system was developed and proposed. This algorithm is presented in the Thesis. Based on the obtained algorithm, software has been developed that allows making calculations of the EPT cooling system parameters with variation of the initial data and boundary conditions.

6. TESTING AND VALIDATION OF THE RESULTS. EXPERIMENTS WITH A BASIC PROTOTYPE WITHOUT A COOLING SYSTEM

Two groups of experiments were performed to confirm the validity and verification of the scientific principles and results obtained from the research done regarding the correctness of the proposed approach to modeling and designing the EPT cooling system and its efficiency.

In the framework of the first group of experiments, a Magneto Plasma Dynamic EPT was manufactured and was tested with its own magnetic field without a cooling system. The second group of experiments was performed for the EPT with a switchable external magnetic field and with a cooling system, which was designed based on the proposed model calculation.

In both cases, the thrusters had the same geometric characteristics of the electrode system.

For the experiments, a special facility and a test bench was designed and produced. To do this, their parameters were calculated. The description of the special facility and the test bench is given in the appendix of the Thesis.

The objectives of the first group of experiments were:

1. Evidence of electro thermal failure possibility of EPT with a power of more than 1 kW.
2. Proof of a cooling system needed for EPT with a power of more than 1 kW.
3. Data collection for designing an EPT cooling system.

For the experiment, a coaxial Magneto Plasma Dynamic EPT with its own magnetic field without a cooling system (hereinafter MPDO) was manufactured. The EPT already mentioned in this Thesis was adopted as the basis of the developed MPDO [14], which, proceeding from the goals of the study, was substantially modernized.

Based on the operating conditions of the thruster in atmosphere, not in vacuum, the mechanisms of initial ionization, thruster start-up and supply of the working fluid were changed.

In order to extend the lifetime of the electrode system of the thruster, heavy inert gas argon was used as the working fluid for the EPT. The experimental MPDO diagram is shown in Fig. 6.1.

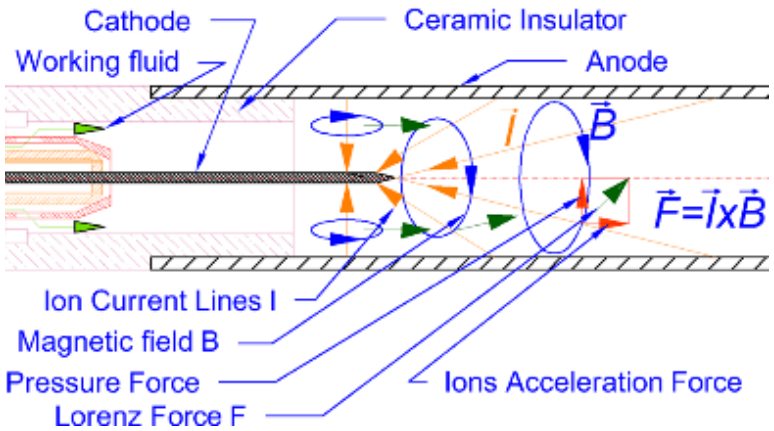

Fig. 6.1. Diagram of experimental MPDO.

The flow of the working fluid enters the ionization zone between the anode and cathode of the experimental MPDO. Initially, the electron impact ionization mechanism consists of only a part of the electrons, scattering from the main trajectory from the cathode to the anode, but as they enter the inter-electrode space, the neutral atoms of the working fluid fall into the main plasma electron flux and the degree of ionization of the working fluid increases. The conductivity of the plasma of the working fluid increases with increasing degree of ionization. As the conductivity increases, current $\boldsymbol{I}$ flowing through the plasma increases, and therefore the magnetic field $\boldsymbol{B}$ and the induced current flowing through plasma. As the current amount $\boldsymbol{I}$ and magnetic field strengths $\boldsymbol{B}$ are increasing in plasma, the Lorenz force $\boldsymbol{F} = \boldsymbol{B} \times \boldsymbol{I}$, acting on plasma ions, also is increasing and hence the ions acceleration is a result. Outside the coaxial portion of the electrode system (as by move toward the cut of the thruster nozzle), the Lorentz force vector begins to rotate in the direction to the thruster axis, and then the vector of Lorentz force resolves into two components: the ions accelerating force, and the compression force, increasing the ions flux compression. The share of compression force increases in the direction from the cathode to the nozzle exit.

Ten experiments were performed using different values of current force and working fluid flow.

Nine of the experiments ended with thermal destruction of the anode. For each new experiment, a new copper anode of the same diameter, thickness, and length was manufactured with the same technological tolerances: in diameter ±0.1 mm, in thickness ±0.1 mm, in length ±0.25 mm. The tenth experiment was devoted to finding the boundary of ignition of an arc discharge due to current value and flow of the working fluid. The flow was regulated by the gas pressure reducing regulator control handle, and the current was controlled by the power supply current limiting handle, which have low installation accuracy, for this reason, the boundary of ignition of a stable discharge was determined conditionally (the discharge ignites and goes out, flashes occur, but there is no stable burning). As a result of numerous switch-on, the tenth anode also received a through defect.

In the process of experiments, the magnitude of following parameters were controlled: discharge current and voltage; current, voltage and power of electromagnets; working fluid flow; coolant temperature and coolant pressure; thrust. The temporal references of experiments were made on photographs and video.

The experimental results are presented in Table 6.1. The table shows the instrument readings, rounded taking into account the measurement of scale error.

The first four experiments were aimed at obtaining data on MPDO thruster operation in maximum thrust mode. The average thrust was 4.7 mN. The average resource before thermal destruction was 11.75 s.

Then six more experiments were carried out, with the following objectives.

1. To identify the possibility of achieving a stable operation of the thruster without a cooling system with a longer resource, to bring the operating lifetime to more than a minute.

2. To determine the maximum resource of the thruster and the boundaries of the stable operation of the thruster by magnitude of current, voltage, discharge power and flow of the working fluid.

Table 6.1

MPDO Experiment Results

No. of test	Average discharge current, A*	Average discharge voltage, V*	Electric power, W	Argon volume flow, nL/min	Time to the failure, s	Destruction reason	Thrust, mH	Comment
1	136	23.1	3142	1.0	12	Anode overheating	4.6	Maximal thrust
2	138	22.9	3160	1.0	11	Anode overheating	4.8	Maximal thrust
3	135	23.1	3119	1.0	13	Anode overheating	4.5	Maximal thrust
4	139	22.9	3183	1.0	11	Anode overheating	4.9	Maximal thrust
5	108	26.0	2808	0.8	14	Anode overheating	2.9	
6	102	26.9	2744	0.7	14	Anode overheating	2.6	
7	89	28.3	2519	0.6	16	Anode overheating	2.0	
8	78	29.4	2293	0.5	18	Anode overheating	1.5	
9	69	31.7	2187	0.4	20	Anode overheating	1.1	Maximal lifetime
10	≥68	~40	Not operate	≥0.3	Not operate	Not operate	Not operate	Instable discharge

As a result of the experiments, it was found that the anode resource increases with decreasing of discharge current magnitude and power. The maximum lifetime of the anode was obtained at a discharge current value of 70 A and an argon flow rate of 0.4 nL/min. In such conditions the anode lifetime was about 20 s. The discharge power was 2.187 kW. Below the specified value of current, power and flow, the discharge becomes unstable; a stable arc does not ignite.

7. EXPERIMENTS WITH MAGNETO PLASMA DYNAMIC EPT WITH COOLING SYSTEM AND WITH SWITCHABLE EXTERNAL MAGNETIC FIELD

To confirm the proposed methodological manual and algorithm for modeling EPT cooling systems, a Magneto Plasma Dynamic EPT was designed with a cooling system and a switchable external magnetic field (hereinafter – MPDE). In the MPDE, equipped with the cooling system, was used the same electrode system, the same supply system for the working fluid and the power supply system as in the above discussed thruster without a cooling system – MPDO (Section 6).

The MPDE cooling system was designed based on the methodological manual, algorithm, and mathematical model that were designed by the author and described in previous chapters of this Thesis. Modeling and experiments (Section 6) have shown that in a coaxial thruster most thermal energy generated by the arc discharge is acted on an anode, and the destruction of the anode begins to develop in its middle region. Therefore, it is necessary to ensure an efficient cooling of the middle part of the anode, thus it was decided to make a coaxial jacket for the refrigerant flow, which provides efficient removal of excess thermal power from the heat-loaded surface of the anode and efficient cooling of its middle region in particular.

The mathematical model realized as software used information about the geometric data of the anode, the previously calculated value of the supplied thermal power (cooling system load) of 2000 W and the functional dependences of the main characteristics of the refrigerant (water) on temperature (thermal conductivity, specific heat, density, dynamic viscosity) in the range from 273.15 K to 373.15 K. Further, the temperature of the anode wall was calculated depending on the flow rate and the temperature of the refrigerant. The calculation result is shown in Figs. 7.1 and 7.2.

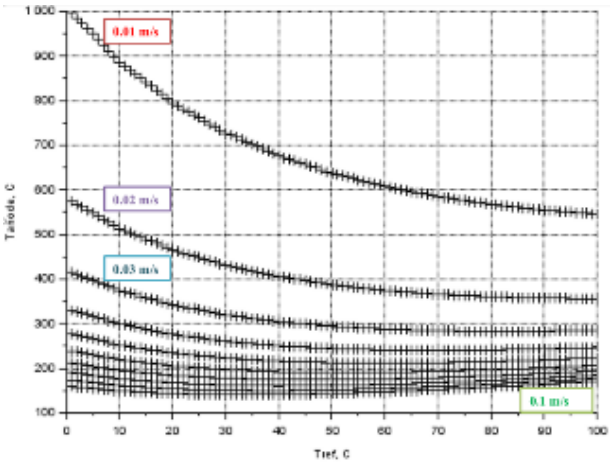

Fig. 7.1. The dependence of the average temperature of the anode on the velocity and temperature of the refrigerant (rough preliminary calculation).

Rough preliminary calculation, the results of which are presented in Fig. 7.1, was carried out in the range of flow rates of the refrigerant from 0.01 m/s to 0.1 m/s in increments of 0.01 m/s and in the temperature range of the refrigerant 0–100 °C (single-phase refrigerant in

the liquid phase). These results show that the range of the safe refrigerant speeds, ensuring the absence of overheating of the anode in the entire temperature range of the refrigerant liquid phase, starts from ~0.015 m/s.

Further, the thruster material properties defining cooling systems design limitations were taken into account: the fact that soldered copper-tin compounds are present on the anode; the upper limit of the operational temperature of the anode was limited to 120 °C. To calculate the refrigerant flow rate satisfying this condition, the more accurate, fine calculation was carried out in the range of refrigerant flow velocities of 0.1–0.5 m/s in steps of 0.05 m/s, the results are presented in Fig. 7.2.

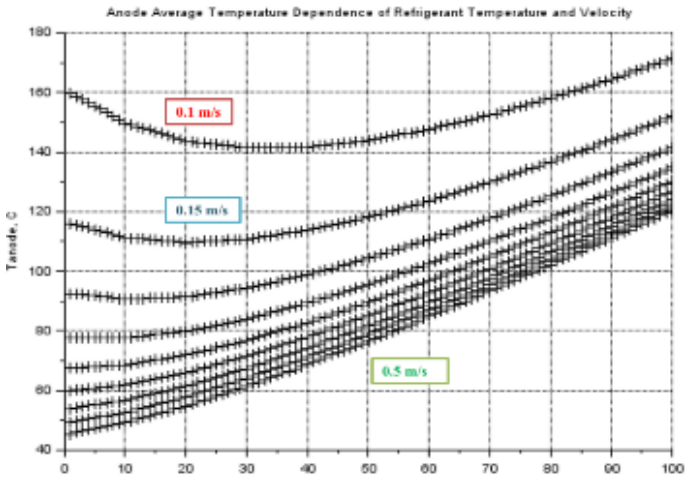

Fig. 7.2. The dependence of the average temperature of the anode on the velocity and temperature of the refrigerant (accurate calculation).

The results of the calculation indicate that the range of refrigerant velocities satisfying the condition of limiting the anode temperature to 120 °C lies above the velocity of ~0.5 m/s.

If it is impossible to reach the indicated velocity with available technical means, then it is necessary to limit the upper range of the operational temperature of the refrigerant, for example to +55 °C at the velocity of 0.15 m/s. Then, the calculation of the refrigerant volumetric flow rate required to ensure a given thermal mode was made. It amounted to $3.004 \cdot 10^{-4}$ m^3/s or 1.08 m^3/h, its mass flow rate was determined depending on its temperature. The results are presented in Fig. 7.3.

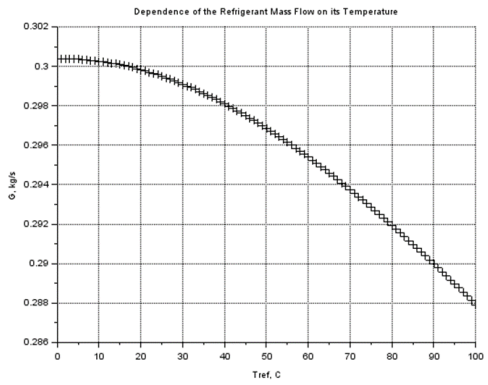

Fig. 7.3. Dependence of the mass flow rate of refrigerant on temperature.

The calculation result shows that it is necessary to take 0.3004 kg/s as the mass flow rate of the refrigerant. The cross-sectional area of the coaxial pipeline of the cooling system was calculated, and based on this, the diameter of the outer tube of the cooling jacket was determined.

Then, the design of the inlet and outlet pipelines for the supply and removal of refrigerant from MPDE anode cavity were performed. Next, the necessary pump head was calculated taking into account hydraulic and local pipeline resistances. For this, the Bernoulli equation in the form proposed in the research was solved. The calculated height of the water column and the required maximum pump pressure value (0.47 MPa) were determined.

The MPDE and its cooling system was designed and calculated using physical and mathematical models, methodological manuals and algorithms developed by the author, and presented in Fig. 7.4.

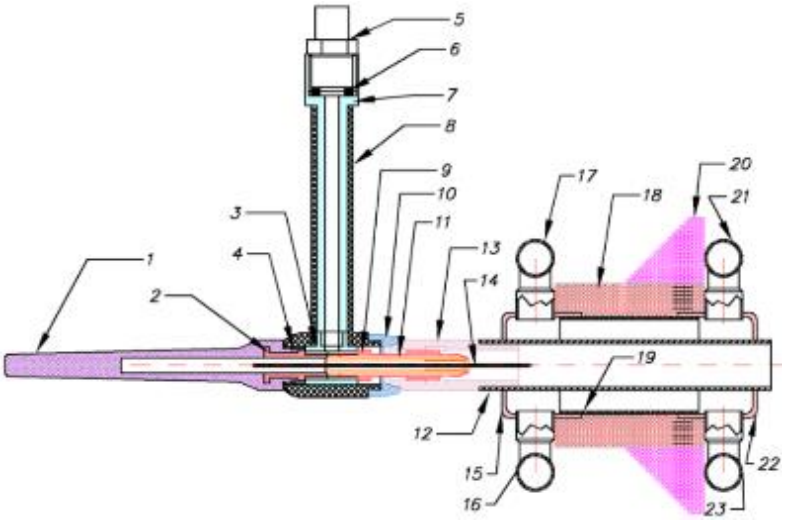

Fig. 7.4. MPDE design developed by the author:

1 – a dielectric concentrator, which serves to transfer the thrust of the MPDE to the strain gauge measuring mechanism, electrical isolation of the cathode system and sealing the cathode cavity; 2 – a brass threaded sleeve around which a dielectric concentrator 1 is printed; 3 – threaded brass coupling-tee into which a dielectric concentrator 1 with sleeve 2 is screwed, a collet clamping cone 9 and pipe 7; 4, 6, 10 – FKM gaskets; 5 – fitting of the argon feed hose, which performs the function of the connector with negative electrode of the thruster; 7 – brass pipe; 8 – silicone case-insulator; 9 – brass clamping cone collet; 11 – collet – cathode holder; 12 – cooled anode – copper tube; 13 – ceramic insulator made of vacuum tight corundum ceramics; 14 – tungsten rod – EPT cathode; 15, 22 – front and rear pipe caps of the cooling cavity of the EPT anode (copper); 16, 17, 21, 23 – fittings for connecting the supply hoses (21, 23) and drain (16, 17) of the coolant; 18 – electromagnet's first coil – an "electron circulation coil", which serves to create a magnetic field, codirectional axis of the thruster; 19 – the outer tube of the cooling cavity of the EPT anode (copper); 20 – electromagnet's second coil "focusing coil", which serves to create heterogeneity of the magnetic field and the implementation of the effect of J. V. Kubarev.

Design of the MPDE cooling system made as a result of modeling

Based on the simulation results, the MPDE cooling jacket was designed with a system of inlet and outlet pipelines hermetically soldered to the anode (Fig. 7.5), which provides effective cooling of the middle region of the anode.

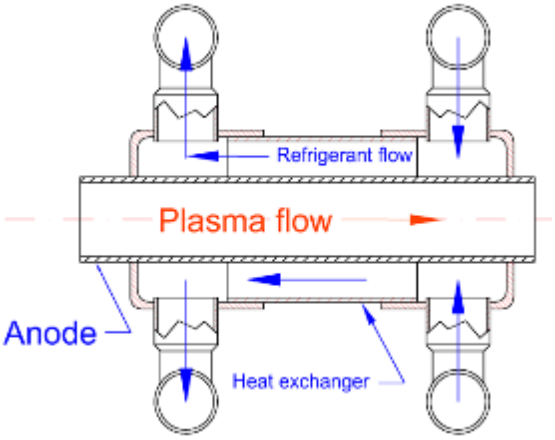

Fig. 7.5. The MPDE cooling jacket design.

Based on the results of mathematical modeling, the MPDE cooling system was developed, which ensures the circulation of coolant through the anode jacket. In this development, a flow-type cooling system with forced circulation of a coolant is used.

Based on the simulation results, a pump with a flow rate of 1 m^3/h was selected, which has a pressure head (maximum height of the pump water column) of 80 m.

The diagram of hydraulic circuit of MPDE cooling system is shown in Fig. 7.6.

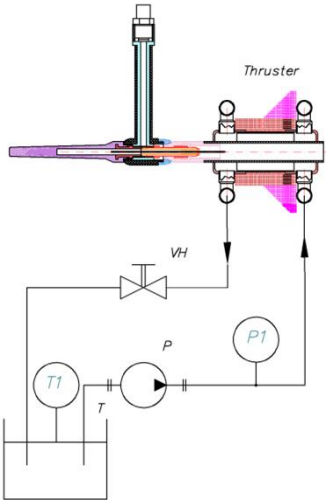

Fig. 7.6. Diagram of hydraulic circuit of MPDE cooling system:
T1 – a thermometer for measuring the temperature of the coolant; T – a tank with coolant; VH – a manual valve that acts as a throttle to maintain the pressure of the coolant in the EPT cooling system; P – an electric pump; P1 – a pressure gauge showing.

The cooling system operates as follows. When power is applied to the electric pump P, it starts to suck in coolant from tank T. From pump P, the coolant under pressure is fed through

a flexible hose system to the nozzles of the EPT cooling jacket from the side of EPT nozzle exit to the atmosphere. Pressure gauge P1 controls the pressure of the supplied fluid. After passing around the outer surface of the MPDE anode, the heated coolant through the outlet pipes and the flexible hose system is fed to the manual valve VH, which acts as a throttle to maintain a given operating pressure in the cooling system. It was necessary to maintain a higher pressure (up to 5.5 bar) in the cooling cavity of the anode in order to remove air bubbles and to prevent the formation of steam jackets due to the near-wall boiling of the refrigerant. After throttling, the coolant flows back to tank T. Tank T has a built-in thermometer T1, which allows determining the temperature rising of the pre-defined volume of the coolant water in the tank. Thus, it is possible to obtain the calculation of thermal losses power of the thruster (taking into consideration that 12.5 liters of water were poured into the tank of the cooling system during the first series of experiments, and then 15 liters of water were poured in addendum).

Analysis of experimental results

1. Experiments with MPDO without the cooling system

1.1. MPDO of such design with a power of more than 1 kW is subjected to electro thermal destruction. Figure 7.7 shows the tendency of increasing thruster lifetime while the electric power is decreasing. For the thruster with such electrode system, a further decrease in power is impossible, since the discharge becomes unstable and the arc does not ignite, but if the inter electrode distance was reduced, such a decrease in power to a certain limit would be possible with a simultaneous increase in thruster lifetime with a corresponding decrease in traction.

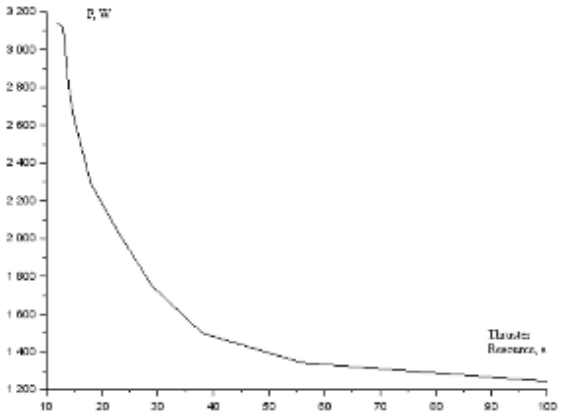

Fig. 7.7. Interpolation of the experiment results to increase the resource by reducing power.

1.2. MPDO with such an electrode system and discharge chamber described above cannot have a resource of more than 20 seconds without the use of the cooling system. Radiation and air-cooling were not effective. This result was verified by repeating 9 experiments. The maximum resource was obtained at a discharge current of 70 A and an argon flow rate of 0.4 nL/min – it was 20 s, and 4 experiments performed in the maximum traction mode without changing the flow rate and discharge current value adjustments showed the thruster lifetime of 11.75 s with a maximum deviation of 8.3 %.

1.3. To assess the correctness of data obtained as a result of tests, a comparison with the calculation results was made. The model proposed by R. G. Jahn for coaxial MPDO [6] was accepted. According to this model, the expression for an ideal full thrust of a coaxial MPDO is

$$F = \frac{\mu I^2}{4\pi}\left[\ln\left(\frac{r_a}{r_c}\right) + \frac{3}{4}\right], \tag{7.1}$$

where μ is magnetic permeability, H/m; r_a is anode radius, m; r_c is cathode radius, m.

In the tested MPDO the anode is a copper pipe with external diameter 18 mm and wall thickness 1 mm, therefore r_a = 0.008 m. The cathode is a tungsten rod, 1 mm diameter, therefore r_c = 0.0005 m. The calculation gives the ideal traction force of 6.6 mN. The ratio of practically obtained thrust to theoretical one is equal to the ratio of theoretical efficiency to practical. The theoretical to experimental thrust ratio is 0.712; average power consumed by the thruster is 3151 W. With a maximum theoretical efficiency of 50 %, the heat loss power would be 1576 W, but the practical efficiency of the thruster is lower, and judging by the ratio of theoretical to practical thrust, it is 35.6 %. Then the heat loss power in the thruster is 2029 W (~2 kW). This value of the thermal power obtained by the calculation corresponds to the value for MPDO determined experimentally, which also confirms their correctness.

1.4. The experiments confirmed the limited lifetime of thrusters without a cooling system. Based on their analysis, the author makes a decision that the causes of overheating and destruction of the thruster anode are electronic bombardment of the anode, which is explained by the following. Since the mass of the negative ion – electron is $5.485\,799\,090\,65(16) \cdot 10^{-4}$ amu and this is near 10^5 times smaller than the mass of the positive ion of argon that is 39.948(1) amu. It means that the electron velocity is near 10^5 times higher than the speed of positive ions of argon in the equal force field of the electrode system. And moreover, the acceleration vector caused by the action of the Lorentz force for electrons has the opposite direction (from the nozzle exit to the influx of a non-ionized working fluid, that is, the electrons "return" to the thruster's acceleration channel). Accordingly, most electrons from the plasma stream bombard the anode and heat it, while positive ions accelerate and leave the thruster, creating reactive thrust.

1.5. The data obtained from the tests allowed the author to formulate initial information for the design of the thruster cooling system:

- The average electric power of the thruster in maximum traction mode is 3151 W, and the average traction is 4.7 mN with an average current of 137 A.
- Since the power of heat losses is the load for the cooling system, the value of 2 kW should be taken as the design input power Q_{in} of the EPT cooling system.

2. Tests of a similar thruster equipped with a cooling system designed in accordance with the model and calculation algorithm, developed by the author

2.1. The total lifetime of the thruster, equipped with a cooling system was 5387 s, which is 406 times higher than the average lifetime of the same thruster without a cooling system. At the same time, at the end of experiments in the MPDO mode, the thruster remained

operational and underwent further tests in the MPDE mode. Operating lifetime in MPDE mode was 4347 s, thus, the total thruster operating resource was 9734 s, which is 734 times greater than the average MPDO resource without a cooling system, while finally the MPDE thruster also remained operational.

2.2. During experiments with the thruster long-term operation, the temperature of the coolant was measured to determine the heat power removed from the electrode system by the cooling system. The results of measurements and calculations are given in Table 7.1.

Table 7.1

Results of Measurements and Calculation of Thermal Power

No. of test	Refrigerant temperature growth, °C	Refrigerant mass, kg	Quantity of heat, received by refrigerant, J	Thruster failure time, s	Heat power received, W	Heat power load, W
5	3.7	12.51	193 618.5	600	322.6975	1936.19
6	3.8	12.51	198 851.5	600	331.4191	1988.51
7	3.9	12.51	204 084.4	600	340.1406	2040.84
8	3.0	15.00	188 235.0	600	313.725	1882.35
9	3.1	15.00	194 509.5	600	324.1825	1945.1
10	28.5	15.00	1788 232.5	1817	984.1676	1949.92

2.3. Analysis of the results show that the average value of the experimentally obtained load power of the cooling system is 1957.15 W and the maximum deviations are within +4.2 % to –1 %.

The estimated load value of the cooling system is 2000 W. The deviation of the obtained average value from the calculated one is 2.1 %, which fits into the general limits of the maximum error of the entire measuring system and test bench (10 %). Thus, the value of the calculated (simulated) thermal load of the cooling system can be considered experimentally confirmed.

3. The experimental results confirm the following

- The fact of a significant increase in thruster lifetime in the presence of a cooling system.
- Determination of correctness of the results obtained by the author: a mathematical model of a cooling system, an algorithm for its calculation and manufacturing technology and their comparison with the results of experiments and comparison with the results of studies of other authors.

SUMMARY AND CONCLUSIONS

1. The Thesis presents theoretical, methodological and experimental approaches for increasing the lifespan (resource) and growing the efficiency of powerful electric rocket thrusters (electric propulsion thrusters, i.e., EPT) based on improving the cooling systems for elements of EPT structures.
2. A methodological manual, a physical and mathematical model, and an algorithm, as well as software for calculating the parameters of the EPT cooling system have been developed.
3. An experimental facility and test bench were designed and made, a series of experiments were performed with a Magneto Plasma Dynamic Ion-Plasma Thruster with its own magnetic field without a cooling system (MPDO) and with a cooling system developed by the author. Based on the analysis of the results of these experiments, the author presented evidence that the cause of overheating and destruction of the thruster anode is electron bombardment of the anode.
4. After calculating, designing and manufacturing the cooling system, which made it possible to multiply the MPDO lifespan, the author made a Magneto Plasma Dynamic Thruster with an External Magnetic Field (MPDE) based on the same electrode system, equipped with the cooling system. This change made it possible to increase the MPDE thrust for the same discharge chamber as the MPDO had by more than an order of magnitude, wherein saving thruster lifetime (resource) also.
5. Practical recommendations have been formulated that can be applied in the design and development of EPTs with cooling systems.
6. The author's findings are based on verification, i.e., comparing the results obtained at several objects and comparing the results obtained by calculations and experiments, as well as assessing the correctness of the experimental results.

Suggestions for further research

For the further development and implementation of EPT cooling systems, according to the author, it is necessary to perform research in two directions:

1. It is necessary to develop and produce a direct-flow type MPDE EPT and a corresponding test facility with an electric power of tens of kilowatts in a continuous mode and megawatts in a pulsed mode using various gases prevailing in the atmospheres of the planets of the Solar system as a working fluid, including atmospheric air. The EPT can use a supercapacitor battery as a pulse- energy storage device, and it is possible to use ethylene glycol and similar reagents as a coolant, which allows achieving an operating range of the heat dissipation subsystem –80 °C to +130 °C, as well as ensuring the integrity of the cooling system during temporary freezing.

   A positive result of research will make it possible to create cruising and correcting spacecraft thrusters with a thrust of hundreds of Newtons in a pulsed mode and a specific impulse in a dense atmosphere of about 500 s and an order of magnitude more

in a rarefied atmosphere, with a resource of hundreds of operation hours. That is, it will make it possible to completely replace chemical engines of the same class with significant savings in spacecraft mass and, thereby, increasing the payload.

2. It is necessary to perform research on the development and manufacture of MPDE EPT with a cryogenic cooling system that uses high-temperature superconducting magnets to create an external magnetic field. Such a thruster can have a power of the order of several megawatts in continuous mode and hundreds of megawatts in pulsed mode, which will make it possible to achieve a thrust of hundreds of kilonewtons in pulsed mode with a specific impulse in vacuum of the order 2000–5000 s and in the atmosphere of the order 500–700 s.

   Research in this direction will make it possible to create the technology, which will be an alternative to environmentally not-friendly chemical rocket engines, with a decrease in the mass of launching systems and spacecraft and an increase in their payload.

REFERENCES

1. Haidn, O. J. Advanced Rocket Engines. In: *Educational Notes RTO-EN-AVT-150, Advances on Propulsion Technology for High-Speed Aircraft*, 2008, Paper 6, pp. 6–40.
2. Isakowitz, S. J., Hopkins, J., Hopkins, J. P. *International Reference Guide to Space Launch Systems.* Reston: AIAA, 2004. 295 p.
3. ESA. *What is Electric propulsion?* Available: www.esa.int/Enabling_Support/ Space_ Engineering_Technology/What_is_Electric_propulsion [Accessed 20.06.2020.].
4. Choueiri, E. Y. A Critical History of Electric Propulsion: The First 50 Years (1906–1956). *Journal of Propulsion and Power,* 2004, vol. 20, no. 2, pp. 193–20. ISSN: 0748-4658. DOI: 10.2514/1.9245.
5. Patterson, M. *Ion Propulsion*. NASA Glenn Research Center, 11.01.2016. Available: https://www.nasa.gov/centers/glenn/about/fs21grc.html [Accessed 20.06.2020.].
6. Bramanti, C., Walker, R., Sutherland, O., Boswell, R., Charles, C., Fearn, D., Gonzalez, J., Orlandi, M. The innovative dual-stage 4-grid ion thruster concept – theory and experimental results. In: *57th International Astronautical Congress proceedings*, Valencia, 2006, IAC-06-C4.4.7, pp. 1–13.
7. ESA. *EPIC: Electric Propulsion Innovation and Competitiveness*. ESA. Available: https://www.esa.int/Enabling_Support/Space_Engineering_Technology/EPIC_Electric_Propulsion_Innovation_and_Competitiveness. [Accessed 20.06.2020.].
8. EPIC. *List of Electric Propulsion Thrusters flown or ordered*. Available: http://epic-src.eu/wp-content/uploads/ Number-of-EP-thrusters-flown-or-ordered_2-1.pdf.
9. Ion and Plasma Rocket Thrusters. In: *Encyclopedia of Low Temperature Plasm*, vol. IV Ed. Academician Fortov, V. E. Moscow: Nauka, 2000, pp. 291–331.
10. EPIC. *Electric Propulsion applications and type of thrusters.* EPIC. Available: http://epic-src.eu/?page_id=63. [Accessed 20.06.2020.].
11. Sovey, J. S., Rawlin, V. K. and Patterson, M. J. Ion Propulsion Development Projects in U. S.: Space Electric Rocket Test 1 to Deep Space 1. *Journal of Propulsion and Power,* 2001, vol. 17, no. 3, pp. 517–526. ISSN: 0748-4658. DOI: 10.2514/2.5806.
12. Arcis, N. *Report D2.1 Database on EP (and EP-related) technologies and TRL*. EPIC, 2015. Available: http://epic-src.eu/wp-content/uploads/EPIC-D2.1-1.2.pdf [Accessed 20.06.2020.].
13. Cassady, R. J., Hoskins, W. A., Campbell, M., Rayburn, C. A micro pulsed plasma thruster (PPT) for the "Dawgstar" spacecraft. In: *2000 IEEE Aerospace Conference. Proceedings*, MT, USA: Big Sky, 2000, vol. 4, pp. 7–14. DOI: 10.1109/AERO.2000. 878359.
14. Ostrovsky, V. G., Smolentsev, A. A., Sokolov, B. A. Experience of High-Power Electric Propulsion at S.P.Korolev Rocket and Space Corporation "Energia". *Electronic journal "Trudy MAI",* 2012, no. 60, pp. 8–26.
15. Gorshkov, O. A., Shutov, V. N., Kozubsky, K. N., Ostrovsky, V. G., Obukhov, V. A. Development of High Power Magnetoplasmadynamic Thrusters in the USSR. In:, *30th International Electric Propulsion Conference*, Florence, 2007, IEPC-2007-136, pp. 1–13.

16. Pencil, E. *Magnetoplasmadynamic Thrusters.* FS–2004–11–022–GRC, Cleveland: Glenn Research Center, 2004. Available: https://www.nasa.gov/centers/glenn/about/fs22grc.html.
17. Blockley, R. and Shyyc, W. Eds. Magnetoplasmadynamic Thrusters. In: *Encyclopedia of Aerospace Engineering*, John Wiley & Sons, Ltd., 2010, pp. 10–11.
18. Institute of heat engeneering. *Gas Resistojet Thruster for Medium Size Satellite Attitude Control*. Web-publication. Warsaw: Institute of heat engineering, 2013. Available: https://www.eng.itc.pw.edu.pl/Pracownicy/Badawczo-dydaktyczni/Mezyk-Lukasz/ Resistojet. [Accessed 20.06.2020.].
19. Surrey Satellite Technology Limited. Available: https://www.sstl.co.uk /Products/Subsystems/Propulsion-Systems/Low-Power-Resistojet. [Accessed 20.06.2020.].
20. Smith, R. D., Aadland, R. S., Roberts, C. R. and Lichtin, D. A. Flight qualification of the 2.2kW MR-510 hydrazine arcjet system. In: *International Electric Propulsion Conference*, Cleveland, 1997, IEPC-97-082, pp. 510–517.
21. Lockheed Martin. *A2100; A2100 Foundation*. Lockheed Martin, 20.06.2020. Available: https://www.lockheedmartin.com/en-us/news/features/history/a2100.html. [Accessed 20.06.2020.].
22. Sercel, J. ECR Thruster Research – Preliminary Theory and Experiments. In: *25th AIAA/ASME/SAE/ASEE Joint Propulsion Conference and Exhibit*, Monterey, 1989. DOI: 10.2514/6.1989-2379.
23. Groh, K. H., Loeb, H. W. State of the art of radio-frequency ion sources for space propulsion. *Review of Scientific Instruments*, 1998, vol. 65, no. 1741, pp. 1259–1259. DOI: 10.1063/1.1145025.
24. Emsellem, G. D., Larigaldie, S. Development of the Electrodeless Plasma Thruster at High Power: Investigations on the Microwave-Plasma Coupling. In: *The 30th International Electric Propulsion Conference*, Florence, 2007, IEPC-2007-240, pp. 1–17.
25. ESA Advanced Concepts Team. *Helicon Radiofrequency Plasma Thrusters.* ESA, 2017. Available: http://www.esa.int/gsp/ACT/projects/helicon/. [Accessed 20.06.2020.].
26. European Comission CORDIS. EU FP7 HPH.com EC Grant Agreement n. 218862 *Final report HeliconPlasmaHydrazine.COmbinedMicro.* EC, 2012. Available: https://cordis. europa.eu/docs/results/218/218862/final1-hph-final-publishable-summary-final.pdf. [Accessed 20.06.2020.].
27. Ad Astra Rocket Company. *Our Engine The Variable Specific Impulse Magnetoplasma Rocket (VASIMR®) engine.* Available: http://www.adastrarocket.com/aarc/VASIMR. [Accessed 20.06.2020.].
28. NASA. *NASA news, june 13, 2000.* Available: https://www.nasa.gov/centers/ %20johnson/news/ releases/1999_2001/h00-91.html. [Accessed 20.06.2020.].
29. Ilin, A. V., Gilman, D. A., Carter, M. D., Chang Díaz, F. R., Squire, J. P. and Farrias, J. E. VASIMR® Solar Powered Missions for NEA Retrieval and NEA Deflection. In: *33-rd International Electric Propulsion Conference*, Washington D.C., 2013, IEPC-2013-336, pp. 1–9.
30. Ad Astra Rocket Company. Press release 03.08.2016. Available: http://adastrarocket.com /pressReleases/AdAstra-Release-080316-final.pdf. [Accessed 20.06.2020.].

31. NASA Glenn Research Center. *Specific Impulse.* NASA GRC, 2018. Available: https://www.grc.nasa.gov/www/k-12/airplane/specimp.html. [Accessed 20.06.2020.].
32. Goebel, D., Katz, I. *Fundamentals of Electric Propulsion: Ion and Hall Thrusters.* Pasadena: Jet Propulsion Laboratory, California Institute of Technology, 2008. 493 p.
33. Jahn, R. G. *Physics of Electric Propulsion.* Mineola: Dover Publications, Inc., 2006. 368 p.
34. Turner, M. J. L. *Rocket and Spacecraft Propulsion: Principles, Practice and New Developments.* Chichester: Springer Praxis Books, 2009. 414 p.
35. Sankovic, J. M., Hamley, J. A., Haag, T. W. Performance Evaluation of the Russian SPT-100 Thruster at NASA LeRC. In: *23rd International Electric Propulsion Conference proceedings*, Seattle, 1993, IEPC-95-30, pp. 246–253.
36. Morozov, A., Soloviev, L. Steady-State Plasma Flow in Magnetic Field. *Reviews of Plasma Physics,* 1980, vol. 8, Ed. Academician Leontovich, M. A., Boston: Springer U.S., pp. 1–103. ISSN 0080-2050. DOI: 10.1007/978-1-4615-7814-7.
37. Golovatiy, Y. *Vacuum and plasma electronics.* Kaluga: Bauman MSTU Kaluga branch, 2007. 328 p.
38. Morozov A. I., Savelyev V. V. Fundamentals of Stationary Plasma Thruster Theory. *Reviews of Plasma Physics*, 2000, Vol 21, Boston: Springer, pp. 203–391. DOI: 10.1007/978-1-4615-4309-1_2.
39. Chen, E. *Applied Phisics - 2. Thin Film Deposition.* Harvard: Harvard University, 2004. Available: https://www.mrsec.harvard.edu/education/ap298r2004/Erli%20chen Fabrication%20II%20-%20Deposition-1.pdf. [Accessed 20.06.2020.].
40. Zhunda, A. N., Veretin, M. I., Pomerantsis, J. R., Kats, A. S. *Planar magnetron sputtering apparatus with the cathode length 1800 mm.* In collection of scientific publications Physical vapor deposition, Riga: Zinatne, 1986, pp. 49–52. UDC:621.793.7 : [621.793.12 : 621.52].
41. NASA Glenn Research Center. *Ion Propulsion.* NASA GRC, 17.01.2020. Available: https://www.nasa.gov/sites/default/files/atoms/files/ionpropfact_sheet_ps-01628.pdf.
42. Larigaldie, S. *Plasma thruster and method for generating a plasma propulsion thrust.* USA Patent US20150020502A1, 22 01 2015.
43. Gordeev, K. G., Ostapushenko, A. A., Galaiko, V. N., Volkov, M. P. Automatic spacecrafts electro jet propulsion devices power and control systems. *Bulletin of the Tomsk Polytechnic University,* 2009, vol. 315, no. 4, pp. 131–136. ISSN 2413-1830.
44. Gallimore, A. D., Thurnau, A. F. The Physics of Spacecraft Hall-Effect Thrusters. In: *American Phisical Society, 61st Annual Meeting of the APS Division of Fluid Dynamics.* Invited Talks, San Antonio, 2008.
45. Marchandise, F., Dumazert, P., Jolivet, K., Estublier, D., Lazurenko, A., Prioul, M., Vial, V., Bouchoule, A., Lasgorceix, P., Albarède, L., Mazouffre, S., Pagnon, D., Echegut, P. PPS-1350 Qualification Status and Performances. In: *Proceedings of the 4th International Spacecraft Propulsion Conference*, (ESA SP-555), 2–9 June 2004, Chia Laguna (Cagliari), Sardinia, Italy, pp. 1–34. Available: http://adsabs.harvard.edu/full/ 2004ESASP.555E..34P.

46. Metghalchi, K. E. F. H., Keck, J. C. Thermodynamic Properties of Ionized Gases at High Temperatures. *Journal of Energy Resources Technology,* 2011, vol. 133, NY: ASME, 2011. pp. 022201–022201. ISSN 0195-0738.
47. Winter, M. W., Auweter-Kurtz, M., Pfrommer, T., Semenova, N. Plasma Diagnostics on Xenon for Application to Ion Thrusters. In: *29th International Electric Propulsion Conference,* Princeton, 2005, IEPC-2005-079, pp. 1–11.
48. Ahedo, E., Gallardo, J. M., Martınez-Sanchez, M. Model of the plasma discharge in a Hall thruster with heat conduction. *Physics of plasmas,* 2002, vol. 9, no. 9, pp. 4061–4070. ISSN 1070-664X. DOI: 10.1063/1.1499496.
49. Kline, J. L. *Slow wave ion heating and parametric instabilities in the HELIX helicon source.* Dissertation submitted for the degree of Doctor of Philosophy in Plasma Physics. West Virginia University, Morgantown, 2002. Available: https://researchrepository. wvu.edu/cgi/viewcontent.cgi? article=2595&context=etd.
50. Kline, J. L., Scime, E. E., Boivin, R. F., Keesee, A. M., Sun, X., Mikhailenko, V. S. Rf Absorption and Ion Heating in Helicon Sources. *Phisical Review Letters,* 2002, vol. 88, no. 19, pp. 195002–195002.4. ISSN 0031-9007. DOI: 10.1103/PhysRevLett.88.195002.
51. Safran. *PPS®1350-G plasma thruster*. Safran, 20.06.2020. Available: https://www. safran-aircraft-engines.com/space-engines/satellites/pps-1350-g. [Accessed 20 06 2020].
52. Kubarev, J. V. *The nature of appearance of electrostatic instability of plasma moving in inhomogenic electric and magnetic fields*. USSR State Register of Discoveries, Diploma No 14, 04 12 1963.
53. Brown, D. L. *Investigation of low discharge voltage hall thruster characteristics and evaluation of loss mechanisms.* A dissertation submitted in fulfillment of the requirements for the degree of Doctor of Philosophy (Aerospace Engineering), University of Michigan, Ann Arbor, 2009. Available: https://deepblue.lib.umich.edu/handle/ 2027.42/63660.
54. Morozov, A. I., Bugrova A. I., Maslennikov, N. A. Laws of similarity of integral characteristics of UZDP. *Technical Physics,* 1991, vol. 61, no. 6, pp. 45–52. ISSN: 0044-4642. Moscow: Russian Academy of Science. Available: https://journals.ioffe.ru/articles/ 24622.
55. Dannenmayer, K. *Scaling laws and electron properties in Hall effect thrusters.* Docctoral thesis. Université d'Orléans, 2012. Available: https://tel.archives-ouvertes.fr/tel-00797732/document.
56. Incropera, F. P. *Fundamentals of Heat and Mass Transfer.* New-York: John Willey & Sons, 2011.
57. Ekuoe, F., Fouache d'Halloy, A., Gigon, D., Plantamp, G., Zajdman, E. Maxwell-Cattaneo Regularization of Heat Equation. *International Journal of Mathematical, Computational, Physical, Electrical and Computer Engineering,* vol. 7, pp. 772–775, 2013. Available: https://publications.waset.org/3892/pdf.
58. Christov, C. I. On frame formulation of the Maxwell-Cattaneo model of finite-speed heat conduction. *Mchanics Research Communications,* 2009, vol. 36, iss. 4, pp. 481–486. DOI: 10.1016/j.mechrescom.2008.11.003.

59. Mariano, P. M. Finite speed heat propagation as a consequence of microstructural events. In: *14 Joint European Thermodynamics Conference Proceedings*, Budapest, 21–25 May 2017. Available: http://jetc2017.hu/wp-content/uploads/2017/03/MinisympH3.pdf.
60. Jensen, J. E., Tuttle, W. A., Stewart, R. B., Brechna, H., Prodell, A. G. *Brookhaven National Laboratory Selected Cryogenic Data Notebook*. Associated Universities, INC., 1980. Available: https://www.bnl.gov/magnets/Staff/Gupta/cryogenic-data-handbook/index.htm.
61. Idelchik, I. E. *Handbook of Hydraulic resistance*. New York: Begell House, 2008. 861 p.
62. Altschul, A. D. *Hydraulic resistance*. Moscow: Nedra, 1982. 224 p.
63. Bashta, T. M. *Engineering Hydraulics*. Moscow: Mashinostroenie, 1971. 678 p.
64. EN 10 088-2:2014 E, Stainless steels – Sheet/plate and strips for general purposes, European Committee for Standardization, 2014.
65. EN 10 088-3:2014 E, Stainless steels. – Technical delivery conditions for general purpose semi-finishedproducts, bar, rod and sections, European Committee for Standardization, 2014.
66. EN 10 296-2:2005, Welded circular steel tubes for mechanical and general engineering purposes – Part 2: Stainless steel, European Committee for Standardization, 2005.
67. EN 10 297-2:2005, Seamless circular steel tubes for mechanical and general engineering purposes – Part 2: Stainless steel, European Committee for Standardization, 2005.
68. ISO 5167-1, Measurement of fluid flow by means of pressure differential devices inserted in circular cross-section conduits running. Annex B: Examples of values of the pipe wall uniform equivalent roughness, Geneva: International Standard Organization, 2003.
69. McGovern, J. *Technical Note: Friction Factor Diagrams for Pipe Flow*. Technological University Dublin, 2011. 16 p. Available: https://arrow.tudublin.ie/engschmecart/28/.
70. National Oceanic and Atmospheric Administration, NASA, USAF. *U.S. Standart Atmosfere, 1976*. Washington: U.S. Government Printing Office, 1976.
71. Kubarev, J. V. *Gas-discharge source of low-temperature plasma with oscillating electrons*. USSR Patent 196198, d.d. 29.10 1963.
72. Kubarev, J. V. *Source of gas-discharge plasma*. USSR Patent 166974, d.d. 12.12.1964.